

AN EXPERIMENTAL EVALUATION OF A FREE-FLOATING  
SUPERCONDUCTING SOLENOID AS A LOW-LEVEL ACCELEROMETER

by

EDWARD AMES HILDUM

Submitted in Partial Fulfillment

of the Requirements for the

Degree of Bachelor of Science

at the

MASSACHUSETTS INSTITUTE OF TECHNOLOGY

June, 1979

Signature of Author *E. A. Hildum* .....

Department of Physics, May 22, 1979

Certified by *N.* .....

Thesis supervisor

Accepted by .....

Chairperson, Departmental Committee on Theses

ARCHIVES  
MASSACHUSETTS INSTITUTE  
OF TECHNOLOGY

JUN 28 1979

LIBRARIES

AN EXPERIMENTAL EVALUATION OF A FREE-FLOATING  
SUPERCONDUCTING SOLENOID AS A LOW-LEVEL ACCELEROMETER

by

EDWARD AMES HILDUM

Submitted to the Department of Physics  
on May 22, 1979 in partial fulfillment of the  
requirements for the Degree of Bachelor of Science.

ABSTRACT

This paper examines the feasibility of using a superconducting solenoid as the sensing element of a low-level accelerometer. The resonant frequency of this instrument is 1 Hz along its primary axis and between 5 and 10 Hz on other axes. Its  $Q$  is between 10 and 40 in LHe, and about 65 in gaseous He. In addition, the paper describes the details of construction of the instrument.

Rainer Weiss, Professor of Physics

TABLE OF CONTENTS

Page

2.....Abstract  
4.....Motivation  
5.....Preliminary Calculations  
15.....Experimental Apparatus  
27.....Force vs. Height and Distance Experiment  
35.....Final Apparatus Design  
39.....Resonance and Q Experiments  
46.....Q and Resonance Data Analysis  
49.....Conclusions  
51.....Acknowledgements  
52.....References

### Motivation

Many experimental problems, notably the detection and identification of gravitational radiation, require test platforms which are extremely stable and well isolated from ground noise. For many purposes, it is sufficient to eliminate only the higher frequency components of the ground noise. In these cases, heavy bases are supported on suitably damped springs or air cushions. Systems of this form are practical down to frequencies of a few Hz. Below this range, some form of servo stabilization is more desirable. The elements of this servo system are the base itself, some device capable of moving the base in response to an applied signal, and an accelerometer capable of sensing the motion of the base. This paper will describe the development, and evaluate the utility of a magnetically suspended superconducting solenoid as a low-level accelerometer potentially useful in such a servo system.

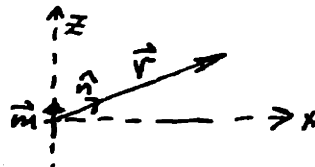
Several considerations suggest a superconducting magnetic suspension as an optimal accelerometer. The absence of ohmic loss in bulk superconducting material allows high suspension Q's and restricts the coupling between the sensing element and its surroundings. It is, in principle, possible to construct a system whose major source of loss and coupling to the external heat bath is the sensor which measures the position of the test mass. It may be possible to build an accelerometer whose sensitivity is limited by the effective noise temperature of the position-sensing electronics. Also, since the forces involved are highly directional, it is possible to construct suspensions which are tightly bound in some directions, but very weakly bound in others. This allows low resonance frequencies, and therefore high low-frequency response, in the weakly bound directions.

### Preliminary Calculations

Previous work by S. Ezekiel<sup>1</sup> in his master's thesis was the primary motivation for the geometry of this experiment. His thesis describes a low level accelerometer in which the sensing element is an Alnico bar magnet floating on its own field inside a niobium tube. The position of this bar magnet is measured interferometrically, and its oscillations are damped by eddy currents in a copper sleeve inside the niobium tube. The disadvantage of this system is that any time varying fields in the tube cause eddy current losses in the bar magnet. Even if the bar remained stationary, there would still be fields caused by thermal motion of the electrons in the copper tube. The resulting eddy current losses would couple the bar magnet to the surrounding heat bath. The ultimate sensitivity of this instrument is therefore limited by the noise temperature of the copper tube.

In the experiments described in this paper, the bar magnet has been replaced by a superconducting solenoid, and the copper-lined tube by a niobium trough (see fig. 1). If this system is to function, the solenoid must produce a magnetic field (resulting in a force) at the surface of the trough sufficient to support its weight. Since the superconductor behaves as a perfect diamagnet, the solenoid field is reflected in the surface of the trough. The resultant forces may be calculated from the interaction between the solenoid and its image. By considering the repulsion between two point dipoles, it is possible to get a crude idea of the forces and currents required. Consider a dipole with magnetic moment  $\vec{m}$ . Then:

$$\vec{B} = \frac{3\hat{n}(\hat{n}\cdot\vec{m}) - \vec{m}}{|\vec{r}|^3},$$



$$\vec{m} = m_z \hat{z}$$

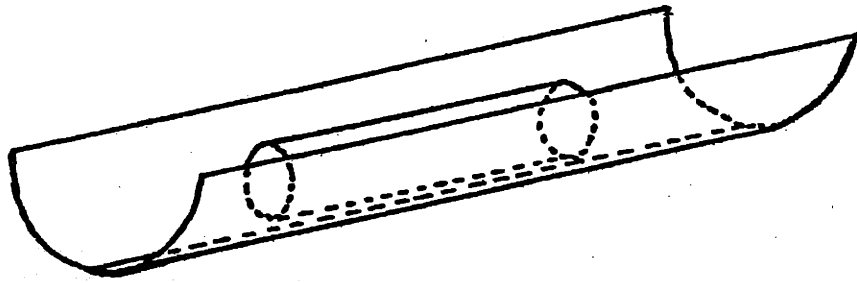


Fig. 1

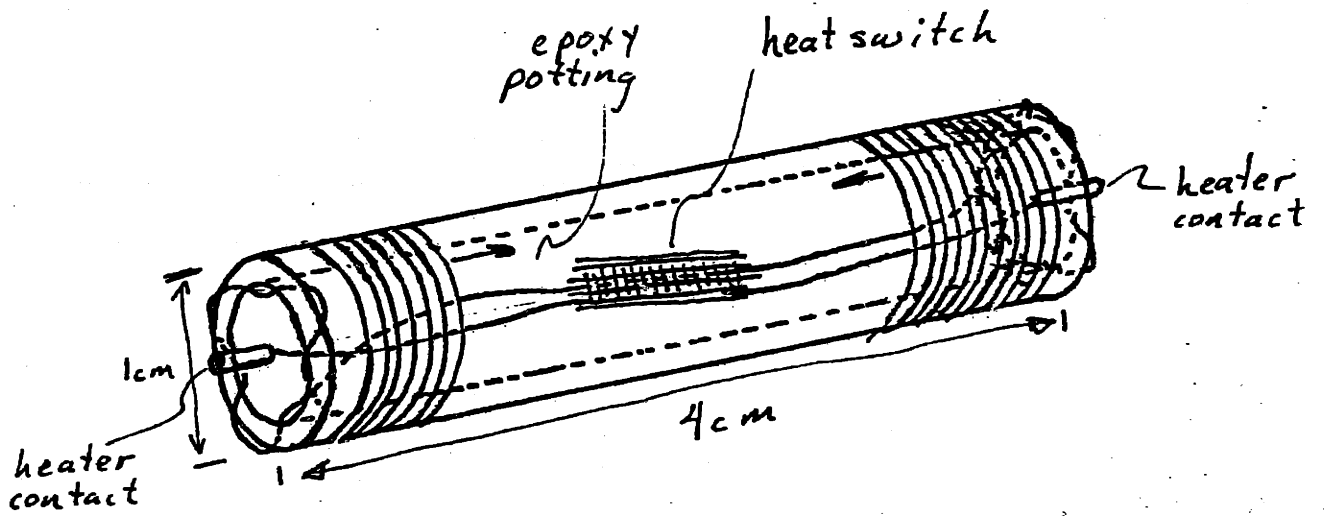


Fig 2

where  $\hat{n}$  is the unit vector along  $\vec{r}$ , the radius vector from the dipole.

Introducing a cartesian coordinate system and simplifying gives:

$$\vec{B} = m_2 \frac{3 \cos^2 \theta - 1}{r^3} \hat{z} + m_2 \frac{3 \cos \theta \sin \theta}{r^3} \hat{x}$$

Taking  $\theta=90^\circ$ :

$$\vec{B} = - \frac{m_2}{x^3} \hat{z}$$

The force on the second dipole in the non-uniform field of the first is:

$$\vec{F} = \vec{\nabla}(\vec{m} \cdot \vec{B}) = \vec{\nabla}(m_z B_z)$$

The x component of this force is:

$$F_x = m_z \frac{\partial B_z}{\partial x} = \frac{3m_z^2}{x^4}$$

Since a small system is desirable, take x as 1 cm. and  $F_x$  as 10000 dyne.

Then:

$$m = 57 \text{ esu-cm}$$

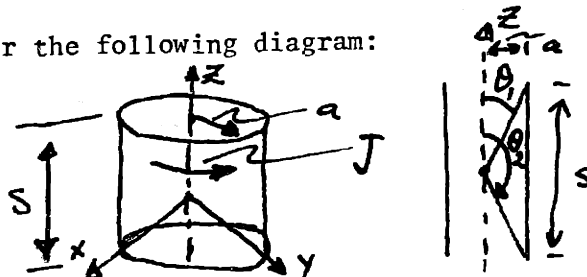
For a small current loop,  $m=Ia/c$ , where I is the current in the loop, a is the area of the loop, and c is the velocity of light. For a 1 cm. diameter loop, the current required to give  $m=57 \text{ esu-cm}$  is:

$$I = \frac{57 \text{ esu cm} \cdot (3 \times 10^{10} \text{ cm/s})}{\pi (.5)^2 \text{ cm}^2} = \frac{2.2 \times 10^{12} \text{ esu/s}}{735} = 735 \text{ A}$$

Niobium-titanium superconductor has a critical current density of  $9 \times 10^4 \text{ A/cm}^2$  in a 20 kOe applied transverse field.<sup>2</sup> This gives a critical current of 180 A for 10 mil. wire. In fact, according to the Magnetic Corporation of America<sup>3</sup> this is a high estimate, and should be reduced to  $\sim 50-70 \text{ A}$  for 10 mil. wire. Since Nb-Ti wire weighs  $\sim 4 \text{ mg/cm}$ , this suggests that 20 turns of 10 mil. wire will easily carry current

sufficient to levitate the above loop. The above approximation is, however, optimistic in several respects. Firstly, the method of images applies to a superconducting sheet of infinite extent. The expected force is therefore smaller than this calculation predicts. Secondly, current loops are only dipoles in the far field, and the above calculation refers to the near field. Furthermore, this geometry is not realistic, since the loop would not float with its axis parallel to the surface, since that position is unstable.

A more realistic geometry is that of a long, thin solenoid above an infinite superconducting plane. This geometry, while still an approximation, should give a better prediction of the actual behavior of the system. Consider the following diagram:



A solenoid is, for the purposes of this calculation, equivalent to a cylindrical current sheet with a uniform surface current density  $J$ , where:

$$J = I_g \delta(r \sin \theta - a) \quad \theta_1 \leq \theta \leq \theta_2$$

To evaluate the constant  $g$ ,

$$I = I_g \int_{\theta_1}^{\theta_2} \int_0^{\infty} \delta(r \sin \theta - a) r dr d\theta$$

using  $\delta$  function identities:

$$I = I_g \int_{\theta_1}^{\theta_2} \int_0^{\infty} \delta\left(r - \frac{a}{\sin \theta}\right) \frac{r}{\sin \theta} dr d\theta$$

$$I = I_g a \int_{\theta_1}^{\theta_2} \frac{d\theta}{\sin^2 \theta} = I_g a \left( -\cot \theta \Big|_{\cot \theta = \frac{s}{2a}}^{\cot \theta = -\frac{s}{2a}} \right) = I_g s$$



Therefore:

$$g = \frac{1}{s} \text{ and } J = \frac{I}{s} \delta(r \sin \theta - a)$$

The general expression for the magnetic vector potential,  $A$ , is:

$$\vec{A} = \frac{1}{c} \int_{\text{all space}} \frac{\vec{J} \times \hat{r}'}{|\vec{r} - \vec{r}'|} dV$$

Choosing the observation point in the  $x-z$  plane:

$$\vec{A} = A_\varphi \hat{y}$$

where:

$$A_\varphi = \frac{I}{cs} \int_{\text{all space}} \frac{\delta(r \sin \theta' - a)}{|\vec{r} - \vec{r}'|} \cos \varphi' r'^2 \sin \theta' dr' d\theta' d\varphi'$$

substituting the spherical harmonic expansion for  $1/|\vec{r} - \vec{r}'|$ ,

$$A_\varphi = \frac{4\pi I}{cs} \text{Re} \sum_{l,m} \frac{1}{2l+1} Y_{l,m}(\theta, \varphi) \int Y_{l,m}^*(\theta', \varphi') \delta(r' \sin \theta' - a) \frac{r'^l}{r'^{l+1}} e^{i\varphi'} r'^2 \sin \theta' dr' d\theta' d\varphi'$$

where  $Y_{l,m}$  is the spherical harmonic of order  $l, m$ ;  $\vec{r}_<$  and  $\vec{r}_>$  are the lesser and greater of  $\vec{r}$  and  $\vec{r}'$  respectively. The presence of the  $e^{i\varphi'}$  in the

integral means only terms with  $m=1$  will contribute to the integral.

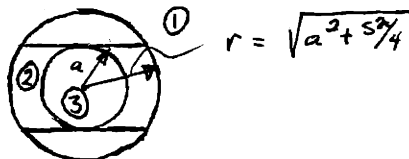
Performing the integration over  $\varphi'$  and evaluating the expression at

$\varphi=0$  gives:

$$A_\varphi(r, \theta, \varphi=0) = \frac{2\pi I}{cs} \sum_l \frac{(l-1)!}{(l+1)!} P_l'(\cos \theta) \int_{r'_<}^{r'_>} P_l'(\cos \theta') \delta(r' \sin \theta' - a) \frac{r'^l}{r'^{l+1}} r'^2 \sin \theta' dr' d\theta'$$

where  $P_l^1(\cos \theta)$  are associated Legendre polynomials of order  $l, m=1$ .

This series has three ranges of interest:



The series converges in regions 1 and 3, but not in region 2, where it is most needed. The most useful convergent region is the far field.

Letting  $r > \sqrt{a^2 + s^2/4}$  and carrying out the integral over  $r'$  gives:

$$A_\varphi = \frac{2\pi I}{cs} \sum_l \frac{(l-1)!}{(l+1)!} P'_l(\cos\theta) \frac{a^{l+2}}{r^{l+1}} \int_{\cot\theta' = \frac{s}{2a}}^{\cot\theta' = -\frac{s}{2a}} P'_l(\cos\theta') \frac{d\theta'}{\sin^{l+2}\theta'}$$

Define:

$$B_l = \int_{\cot\theta' = \frac{s}{2a}}^{\cot\theta' = -\frac{s}{2a}} P'_l(\cos\theta') \frac{d\theta'}{\sin^{l+2}\theta'}$$

These integrals were done by MACSYMA, a symbolic mathematics program

developed by the Mathlab group in the Laboratory for Computer Science.

It turns out that all even  $B_l$ 's are zero. The first eight values of the

odd  $B_l$ 's are given in table 1. The series for  $A_\varphi(r, \theta)$  is then:

$$A_\varphi(r, \theta) = \frac{2\pi I}{cs} \sum_l \frac{(l-1)!}{(l+1)!} P'_l(\cos\theta) \frac{a^{l+2}}{r^{l+1}} B_l$$

$B_r$  and  $B_\theta$  are given by:

$$B_r = \frac{1}{r \sin\theta} \frac{\partial}{\partial\theta} (\sin\theta A_\varphi) = -\frac{1}{r} \frac{\partial}{\partial(\cos\theta)} (\sin\theta A_\varphi)$$

$$B_\theta = -\frac{1}{r} \frac{\partial}{\partial r} (r A_\varphi)$$

Since  $\frac{d}{dx} (\sqrt{1-x^2} P'_l(x)) = l(l+1) P_l(x)$

$B_r$  and  $B_\theta$  can be written:

$$B_r \approx -\frac{2\pi I a^2}{cs r} \left[ \frac{B_1 a}{r^2} P_1(\cos\theta) + B_3 \frac{a^3}{r^4} P_3(\cos\theta) + B_5 \frac{a^5}{r^6} P_5(\cos\theta) \dots \right]$$

$$B_\theta \approx \frac{2\pi I a^2}{cs r} \left[ B_1 \frac{a}{2r^2} P'_1(\cos\theta) + B_3 \frac{a^3}{4r^4} P'_3(\cos\theta) + B_5 \frac{a^5}{6r^6} P'_5(\cos\theta) \dots \right]$$

The pressure exerted on a superconducting surface by the solenoid is:

$$\frac{dF}{dA} = \frac{B^2}{8\pi}$$

Table 1

$$B_1 = -\frac{s}{a}$$

$$B_3 = \frac{3s}{2a} \left(\frac{s}{a}\right)^3$$

$$B_5 = -\frac{15s}{8a} + \frac{15}{8} \left(\frac{s}{a}\right)^3 - \frac{3}{16} \left(\frac{s}{a}\right)^5$$

$$B_7 = \frac{35s}{16a} - \frac{35}{8} \left(\frac{s}{a}\right)^3 + \frac{21}{16} \left(\frac{s}{a}\right)^5 - \frac{1}{16} \left(\frac{s}{a}\right)^7$$

$$B_9 = -\frac{315s}{128a} + \frac{525}{64} \left(\frac{s}{a}\right)^3 - \frac{315}{64} \left(\frac{s}{a}\right)^5 + \frac{45}{64} \left(\frac{s}{a}\right)^7 - \frac{5}{256} \left(\frac{s}{a}\right)^9$$

$$B_{11} = \frac{693s}{256a} - \frac{3465}{256} \left(\frac{s}{a}\right)^3 + \frac{3465}{256} \left(\frac{s}{a}\right)^5 - \frac{495}{128} \left(\frac{s}{a}\right)^7 + \frac{165}{512} \left(\frac{s}{a}\right)^9 - \frac{3}{512} \left(\frac{s}{a}\right)^{11}$$

$$B_{13} = -\frac{3003s}{1024a} + \frac{21021}{1024} \left(\frac{s}{a}\right)^3 - \frac{63063}{2048} \left(\frac{s}{a}\right)^5 + \frac{15015}{1024} \left(\frac{s}{a}\right)^7 - \frac{5005}{2048} \left(\frac{s}{a}\right)^9 + \frac{273}{2048} \left(\frac{s}{a}\right)^{11} - \frac{7}{4096} \left(\frac{s}{a}\right)^{13}$$

$$B_{15} = \frac{6435s}{2048a} - \frac{15015}{512} \left(\frac{s}{a}\right)^3 + \frac{63063}{1024} \left(\frac{s}{a}\right)^5 - \frac{45045}{1024} \left(\frac{s}{a}\right)^7 + \frac{25025}{2048} \left(\frac{s}{a}\right)^9 - \frac{1365}{1024} \left(\frac{s}{a}\right)^{11} + \frac{105}{2048} \left(\frac{s}{a}\right)^{13} - \frac{1}{2048} \left(\frac{s}{a}\right)^{15}$$

Table 2

$$h^{-4}: f_{-4} = -\frac{3}{64} B_1^2$$

$$h^{-6}: f_{-6} = \frac{15}{512} B_1 B_3$$

$$h^{-8}: f_{-8} = -\frac{35}{4096} B_1 B_5 - \frac{175}{16384} B_3^2$$

$$h^{-10}: f_{-10} = \frac{315}{131072} B_1 B_7 + \frac{735}{65536} B_3 B_5$$

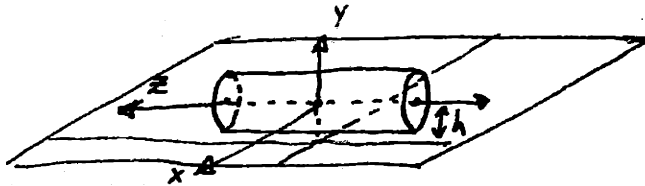
$$h^{-12}: f_{-12} = -\frac{693}{1648576} B_1 B_9 - \frac{10395}{2097152} B_3 B_7 - \frac{4851}{1048576} B_5^2$$

$$h^{-14}: f_{-14} = -\frac{3003}{2^24} B_1 B_{11} + \frac{33033}{2^24} B_3 B_9 + \frac{99099}{2^24} B_5 B_7$$

$$h^{-16}: f_{-16} = -\frac{6435}{2^27} B_1 B_{13} - \frac{195195}{2^28} B_3 B_{11} - \frac{429429}{2^27} B_5 B_9 - \frac{2760615}{2^30} B_7^2$$

$$h^{-18}: f_{-18} = \frac{109395}{2^33} B_1 B_{15} + \frac{546975}{2^31} B_3 B_{13} + \frac{3318315}{2^31} B_5 B_{11} + \frac{15643485}{2^32} B_7 B_9$$

Consider the following figure:



The magnetic field at the surface of the superconducting sheet will be the sum of the field of the solenoid and that of its image. By symmetry, the perpendicular components of the field will cancel and the parallel components will add. The total force on the surface, which is also the force on the solenoid, is:

$$F = 4 \int \frac{B_x^2 + B_y^2}{8\pi} dA$$

Where  $B_x$  and  $B_y$  are:

$$B_x = B_r \sin \theta \cos \varphi + B_\theta \cos \theta \cos \varphi$$

$$B_z = B_r \cos \theta - B_\theta \sin \theta$$

The force integrals were performed by MACSYMA term by term in the distance,  $h$ , from the solenoid axis to the superconducting surface. The first eight terms in the series are compiled in table 2. The force  $F$  is then:

$$F = \frac{4\pi^2 I^2 a^2}{c^2 s^2} \sum_{-2}^{\infty} f_{-2n} \left(\frac{a}{h}\right)^{2n}$$

Table 3 contains the values of the  $f_{-n}$ 's for  $s/a=8$ .

Evaluating  $F$  for  $h=\sqrt{17}$  cm, 5 cm, and 10 cm, with  $a=.5$  cm, and  $s=4$  cm:

$$F(h=\sqrt{17}) \approx -\frac{4\pi^2 I^2 a^2}{c^2 s^2} \left[ 6.79 \times 10^{-4} - 1.819 \times 10^{-4} + 4.64 \times 10^{-5} - 1.10 \times 10^{-5} \right. \\ \left. + 2.32 \times 10^{-6} - 5.04 \times 10^{-7} + 9.91 \times 10^{-8} \dots \right]$$

$$= -\frac{4\pi^2 I^2 a^2}{c^2 s^2} \left[ 5.04 \times 10^{-4} \right]$$

$$F(5) = -\frac{4\pi^2 I^2 a^2}{c^2 s^2} \left[ 2.513 \times 10^{-4} \right]$$

$$F(10) = -\frac{4\pi^2 I^2 a^2}{c^2 s^2} \left[ 1.79 \times 10^{-5} \right]$$

Table 3

$$f_{-4} = -3$$

$$f_{-6} = 57.19$$

$$f_{-8} = -9,913 \times 10^2$$

$$f_{-10} = 1.596 \times 10^4$$

$$f_{-12} = -2.299 \times 10^5$$

$$f_{-14} = 3.420 \times 10^6$$

$$f_{-16} = -4.530 \times 10^7$$

$$f_{-18} = 5.530 \times 10^8$$

Choosing 80 turns of 10 mil. wire for the solenoid, and 10 A solenoid current gives the expected force in dynes:

$$F(\sqrt{17}) \approx - \frac{4\pi^2 I^2 (80)^2 a^2}{c^2 s^2} (5.04 \times 10^{-4}) = 39.48 \cdot I^2 \cdot 5.04 \times 10^{-4} = 1.99 \text{ dyne}$$

(amps)  
for I = 10A

$$F(5\text{cm}) \approx .99 \text{ dyne}$$

$$F(10\text{cm}) \approx .07 \text{ dyne}$$

Taking the value for  $F(\sqrt{17})$  and extrapolating it towards  $h=0$  assuming  $F \propto h^{-4}$  gives a crude idea of the magnitude of the force for smaller values of  $h$ .

$$h = 1\text{cm} \rightarrow F \sim 575 \text{ dyne}, (I = 10A); \sim 2300 \text{ dyne}, (I = 20A)$$

If the force scales in this fashion, this geometry should be feasible. An error in the original calculation gave a value 16 times higher, and construction proceeded from this point.

There are clearly several errors in this approximation. The trough in the actual design is not of infinite extent and is not a plane surface. Since the solenoid is not of infinite extent, the actual force should be some fraction of the calculated value. This fraction should, however, be large, because the force expression peaks so sharply in the vicinity of the coil. On the other hand, the fact that the trough is not a plane should enhance the force since the superconducting surface is closer to the coil.

### Experimental Apparatus

Several factors governed the scale of the coil and trough. The primary constraint was the size of the available LHe dewars, which set the maximum length of the trough at about 9 cm. To improve the approximation of infinite coil extent, the coil should be as small as possible. On the other hand, the mass of the coil scales as the cube of its linear dimensions, while the current carrying capacity of the windings scales as the square of the linear dimensions. Since the Maxwell force goes as the square of the solenoid current, it is advantageous to make the solenoid large. In addition, a larger solenoid is easier to build.

The initial design of the solenoid is shown in fig. 2. The coil is 4 cm long and 1 cm in diameter. The windings are 10 mil. Nb-Ti wire, spaced about .5 mm apart, giving a total of 80 turns. The wire is wound on a threaded hollow nylon form. In the hollow center of the form is a heat switch fastened to the returning loop of the coil. At each end of the coil are exposed portions of Nb-Ti wire intended to form high current contacts for starting the persistent current. Also protruding from the end of the coil are contacts connected to the heater windings. The nylon coil form is made by chucking a length of .5 in. nylon rod in the lathe and drilling a hole through the center (.25 in. to letter M drill). The resulting tube is then jammed on an oversized mandrel and set up on the lathe between centers. From this point, the form is turned down to .4" diam. and threaded with 52 threads per inch. The form is then (gently) removed from the mandrel. Two #75 drill holes are then drilled through the wall of the tube for the ends of the coil windings to pass through. The Nb-Ti wire donated by the Magnetic Corporation of America comes with copper cladding. This copper cladding must be removed by etching

in hot Nitric acid. The end of the wire is then pushed 5 or 6 cm through the small drill hole and the form is returned to the mandrel and chucked in the lathe. This time, the mandrel will only reach to the point where the wire comes through the form wall. The coil is then wound by running the lathe backwards in back-gear and paying out the Nb-Ti wire. Approximately 270 cm of 10 mil wire are required for an 80 turn coil, plus 20 cm for the returning loop and slop at the ends.

Once the coil is wound, the heater must be assembled on the center wire. The Nb-Ti wire is first pulled through the center of the coil so that it protrudes several cm out the far end. The heater windings are electrically insulated from the current windings by a sheet of 10 mil mylar rolled around the wire. To make the mylar roll in this fashion it must be curled. To curl the mylar, a .5" strip several inches long is drawn firmly over a scissors blade (see fig. 4). The curled mylar is easily rolled around the wire to a depth of 2 or 3 layers. The heater coil consists of 1.8 mil Nichrome wire wound around the mylar so that adjacent turns do not touch. The windings should stop about  $\frac{1}{2}$  mm away from the edge of the insulation. To restrict the heat radiated outwards by the heater, the windings are wrapped with layers of aluminized mylar (aluminized side out). The whole assembly is then coated with Epoxy Patch to prevent LHe convection currents from flowing through the heater. When the epoxy hardens, the heater may be slid down the wire into the center of the coil. The heater is shown in fig. 3.

At this point, the ends of the wire must be welded together to close the loop. A superconducting weld may be made by spot welding two parallel wires together at several places along a .25" to .5" joint (see fig. 5). These welds remain superconducting to currents above 20 A,



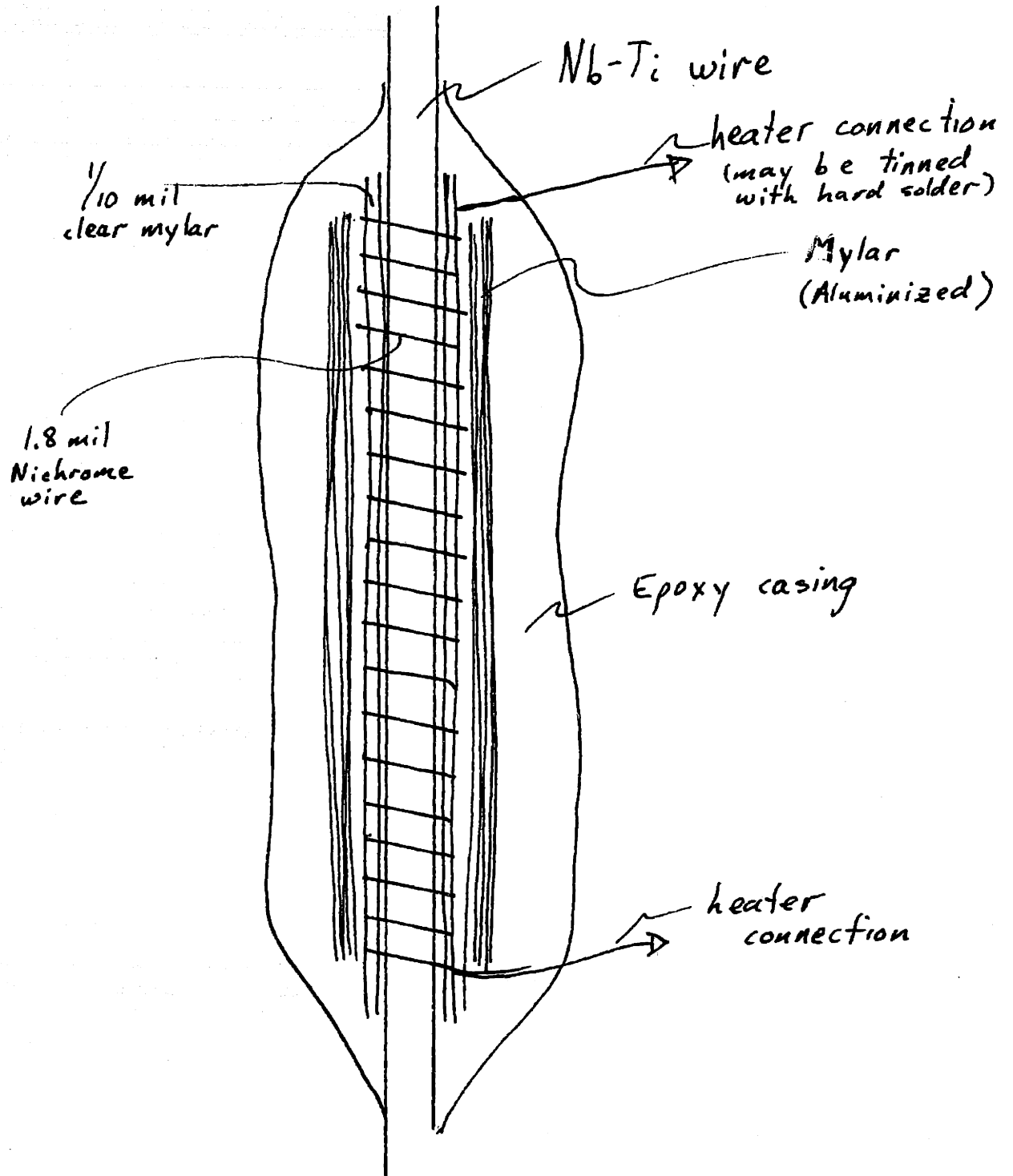


Fig 3

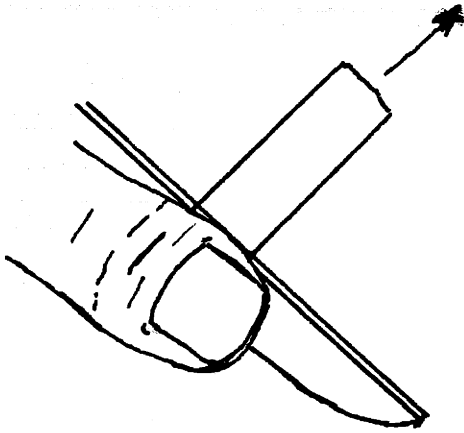


Fig 4

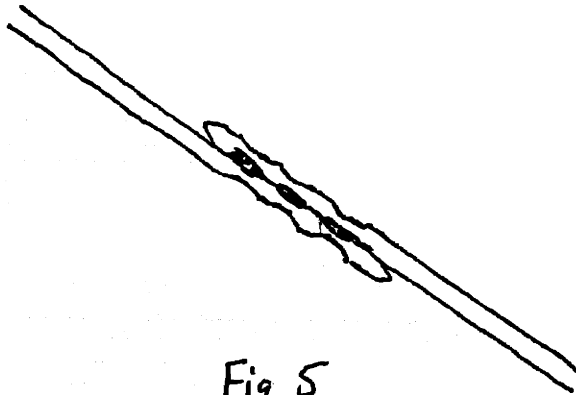


Fig 5

If higher current capacities are necessary, extra lengths of Nb-Ti wire may be welded parallel to the joint. A weld energy of approximately 14 watt-sec appears to make the best welds without destroying the wires. Satisfactory high current (but not superconducting) joints may be made by leaving the copper cladding on the Nb-Ti wire and soldering with ordinary lead-tin solder. These joints will conduct currents above 40 A without driving the wire to its critical temperature.

To establish the current capacities of the heat switch and solenoid, both were immersed separately in LHe. When immersed in LHe, the heat switch plus copper connecting wires had a resistance of about  $.5\Omega$ , as measured by a Data Precision DVOM. With 50 to 70 ma of heater current, the total resistance was  $.7\Omega$ . The current could be switched on and off, and the resistance change would follow. The time required for the heated link to cool down was about 5 sec. A schematic of this test is shown in fig. 6.

In a similar fashion, the coil, with its heat switch, was immersed in LHe. To carry high currents from the room temperature power supply required large copper current leads. These leads consisted of long sections of 12 gauge enameled magnet wire with short lengths of clad Nb-Ti wire soldered into axial holes in their ends. The ends of the Nb-Ti wire were etched and spot welded to the solenoid. With no heater current, the coil assembly would support a current of about 30A. Without quenching. With a heater current of 100 ma, the coil would also support a 30 A current. Above 150 ma, the voltage across the current leads jumped, and the LHe boiled rapidly. Presumably, in this case, the heater drove the whole coil normal. Since the heater could drive the whole coil normal, it was functioning correctly and, at some

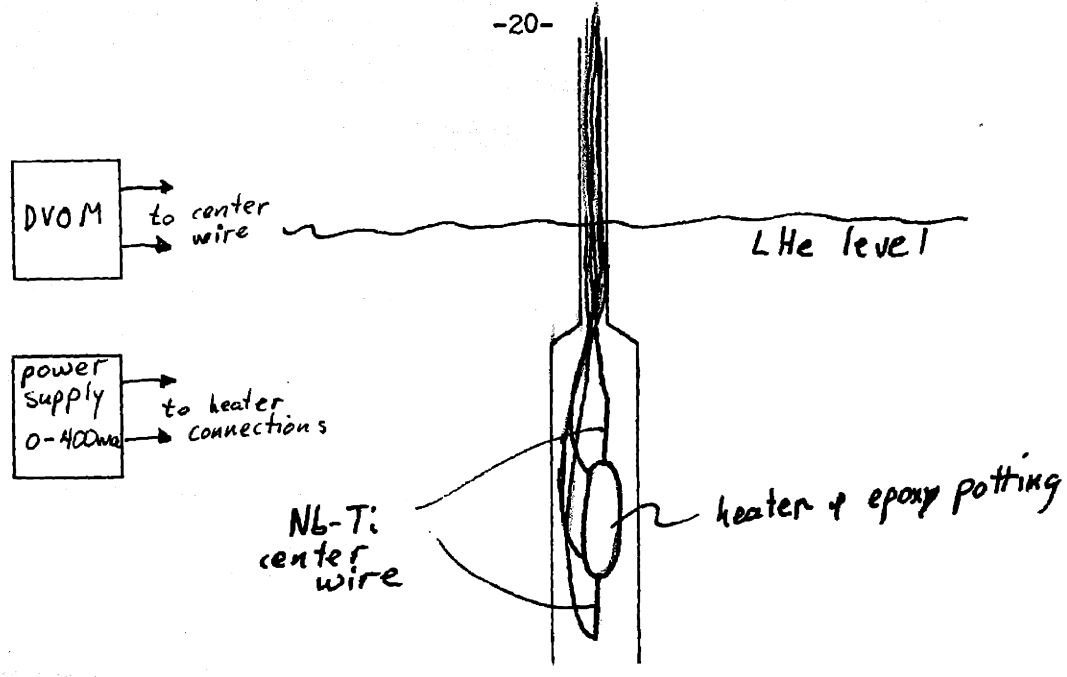
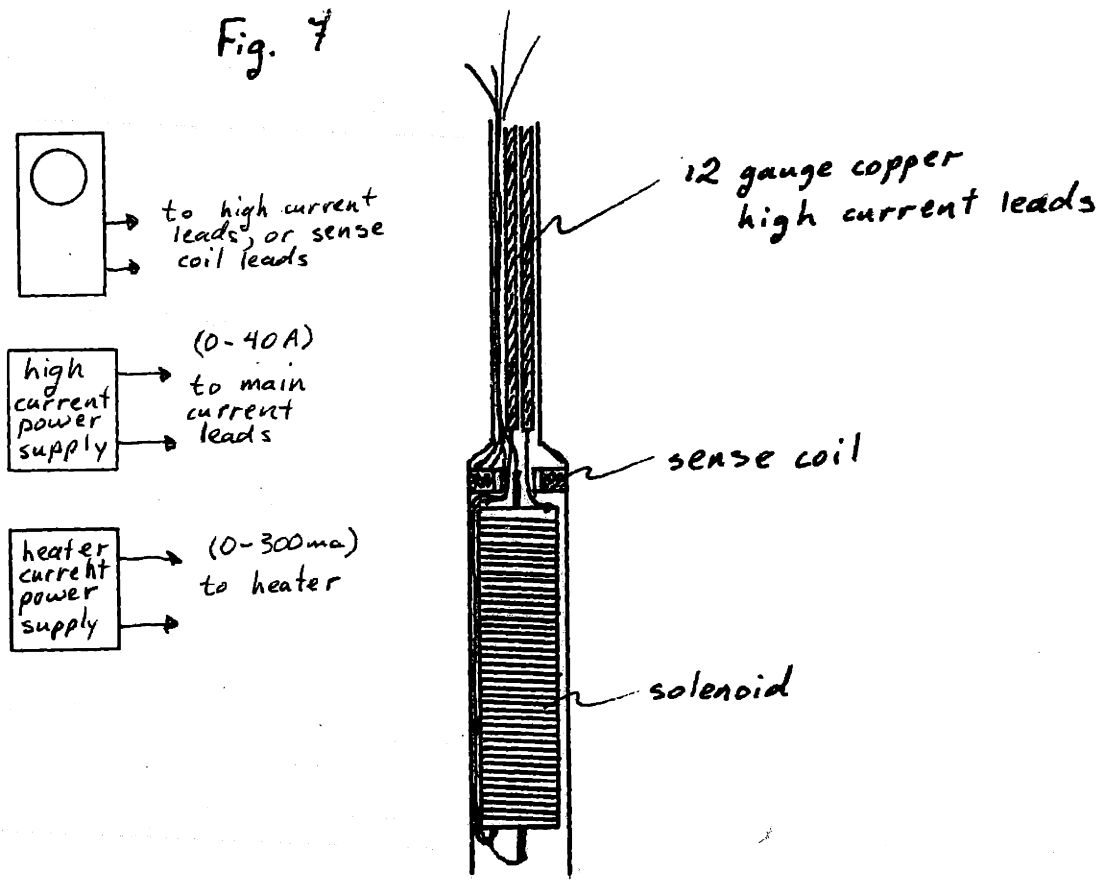


Fig. 6

Fig. 7



point, the outer windings must have been carrying the full current. To make sure a persistent supercurrent could be established, a small sense coil was placed adjacent the solenoid. In this configuration, the sense coil saw the ripple from the power supply when it was on. By looking at the voltage across the sense coil with an oscilloscope, the heater-on and heater-off modes could be distinguished. With the heater off, the power supply spikes were small and rounded. With the heater on, however, the power supply spikes were tall and sharp. Clearly, the higher inductance of the outer windings caused spikes in response to the rapidly changing current. This demonstrated that current actually flowed in the outer windings, rather than the inner link. To show the presence of a persistent supercurrent, the current supply was turned on, the heater turned on and then off, and the current supply turned off. Increasing the heater current produced a sharp spike at a heater current of about 50 ma. This spike did not repeat when the heater was again switched on and off. This clearly indicated the presence of a persistent current which decayed rapidly when the heater drove the center link normal. A schematic of these experiments is in fig. 7.

Further testing required construction of the superconducting trough. The superconducting surface is 15 mil Niobium sheet, cut to the proper (8.6cm x 6.3cm) size with a right-angle sheet metal cutter. Niobium is very ductile, and is easily bent and folded. To obtain the shape shown in fig. 8, the sheet is folded using a mill vise and an aluminum die (fig. 9). A brass base with six uprights supports the Nb sheet. The brass base is fastened to a circular stainless steel plate with four long rods. The stainless plate is, in turn, fastened to a brass top plate with a long stainless steel tube. This arrangement (shown

Fig 8

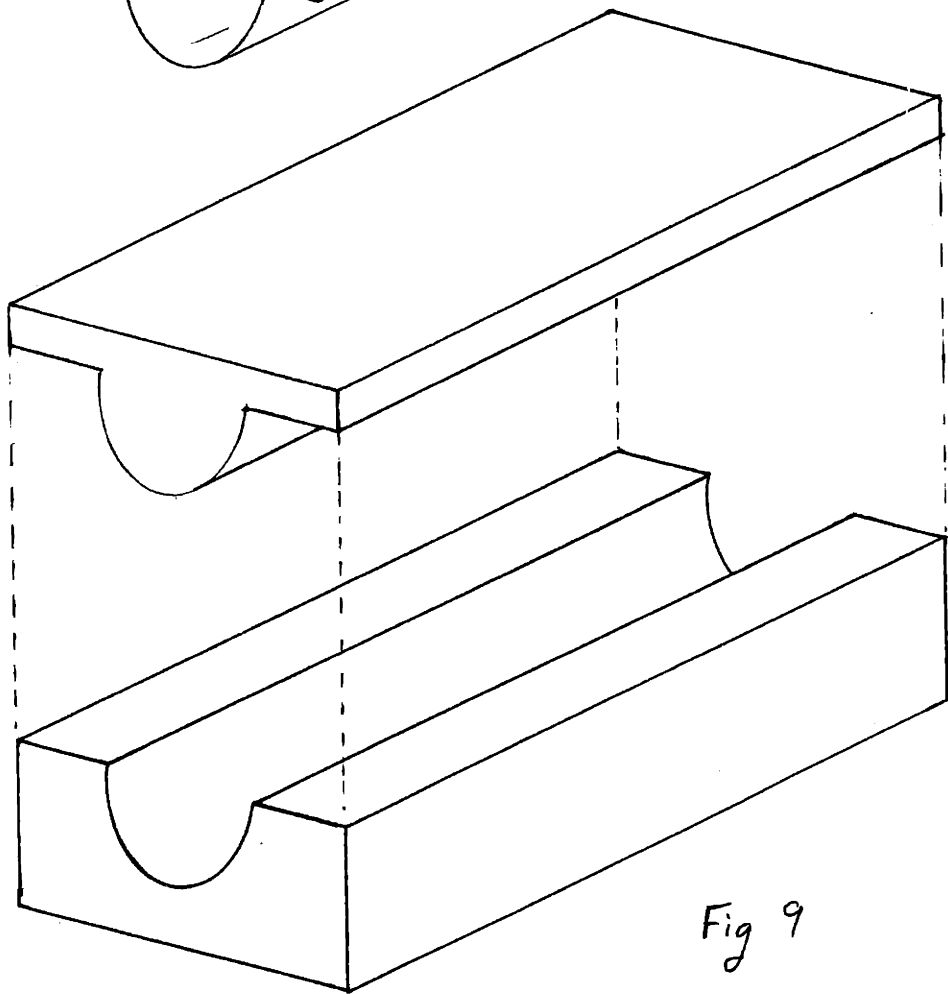
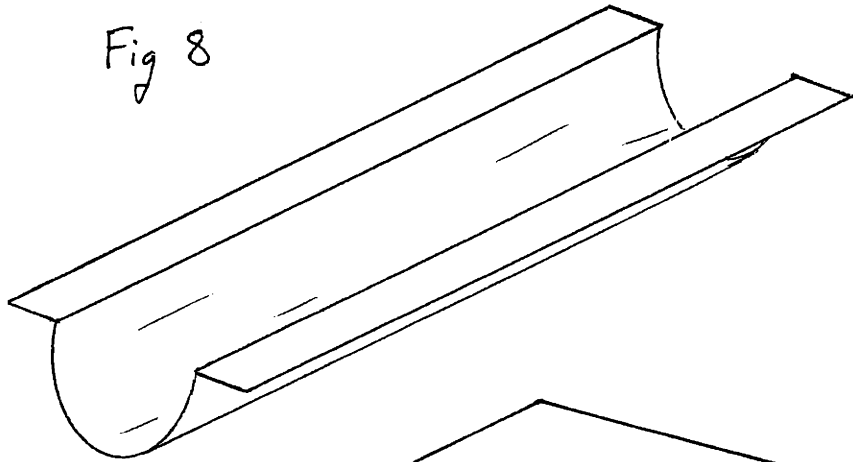


Fig 9

in fig. 10) allows the entire coil assembly to be lowered into a 4" diameter LHe dewar.

To determine whether the solenoid would float on its own field, flexible high current leads and heater connections were attached to the coil. When immersed in LHe, the coil could be excited with a high current from the external power supply while remaining free to move. With 50 ma of heater current, and 25 A solenoid current, the coil jumped to about 2 mm off the surface of the trough. With a 25A persistent current, set up as before, the coil remained floating. This demonstrated conclusively that a 25 A persistent current could be established, and that it would produce a field of the order of size necessary to float the coil. Unfortunately, as was later discovered, a significant fraction of the weight of the coil was supported by the current leads, and the force was not, in fact, sufficient to support that coil.

The next logical step was construction of some sort of device which would grab the coil to start a persistent current, and then release it to float freely. This device consisted of a set of copper cups with spring loaded inner terminals. The copper cups were insulated from the base, and were intended to carry the main solenoid current. The inner terminals, insulated from both the base and the current leads, would carry current to the heater. The entire assembly could be lowered into the trough to grab the coil, and then lifted above the trough to avoid shorting the current leads against the Nb sheet. A drawing of this kluge is in fig. 11. It turned out, ultimately, to be a huge waste of time, and should have been preceded by tests to ascertain whether press contacts would carry sufficient current. In fact, they would not. Subsequent experiments showed that no easily made contacts would carry more

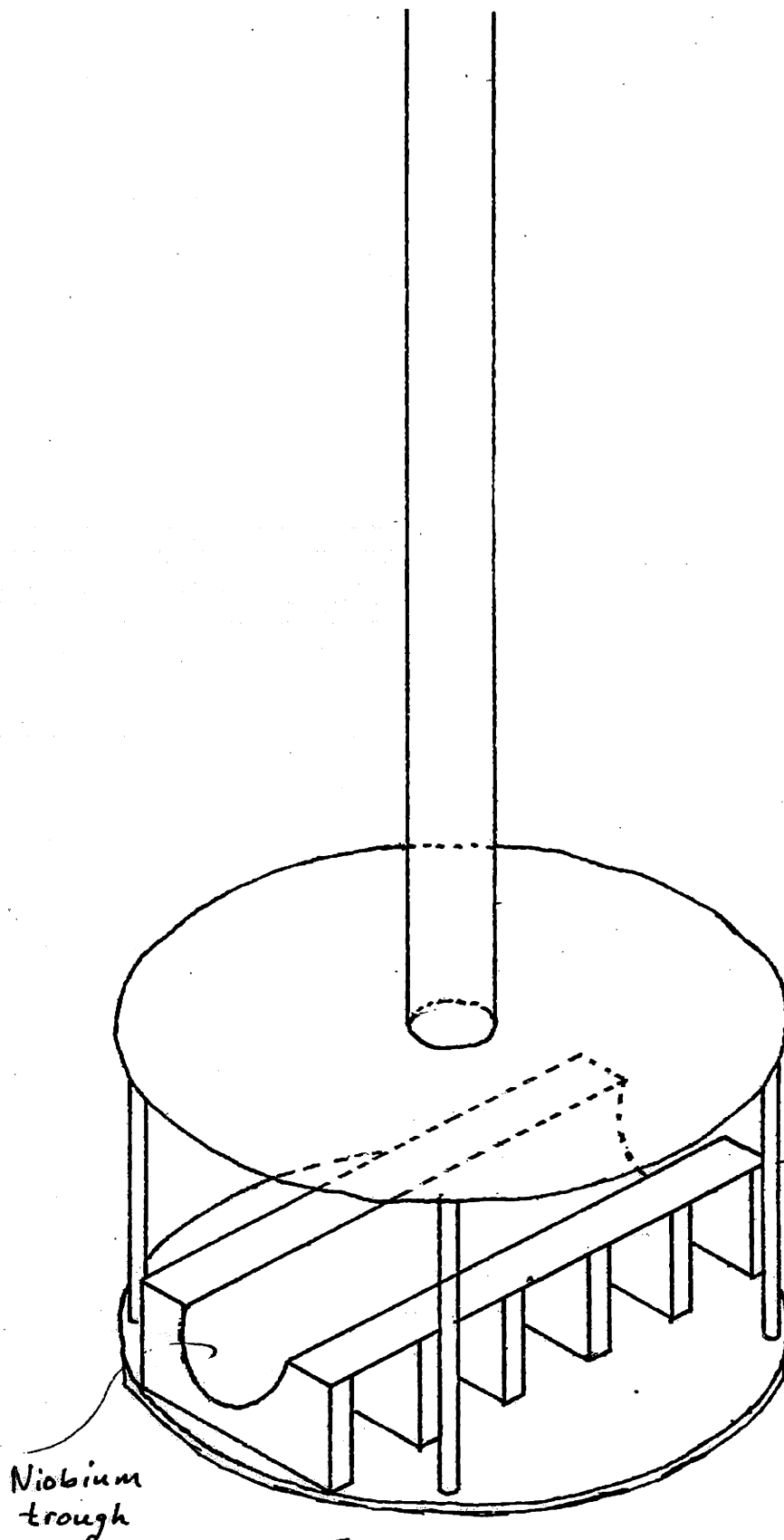


Fig. 10



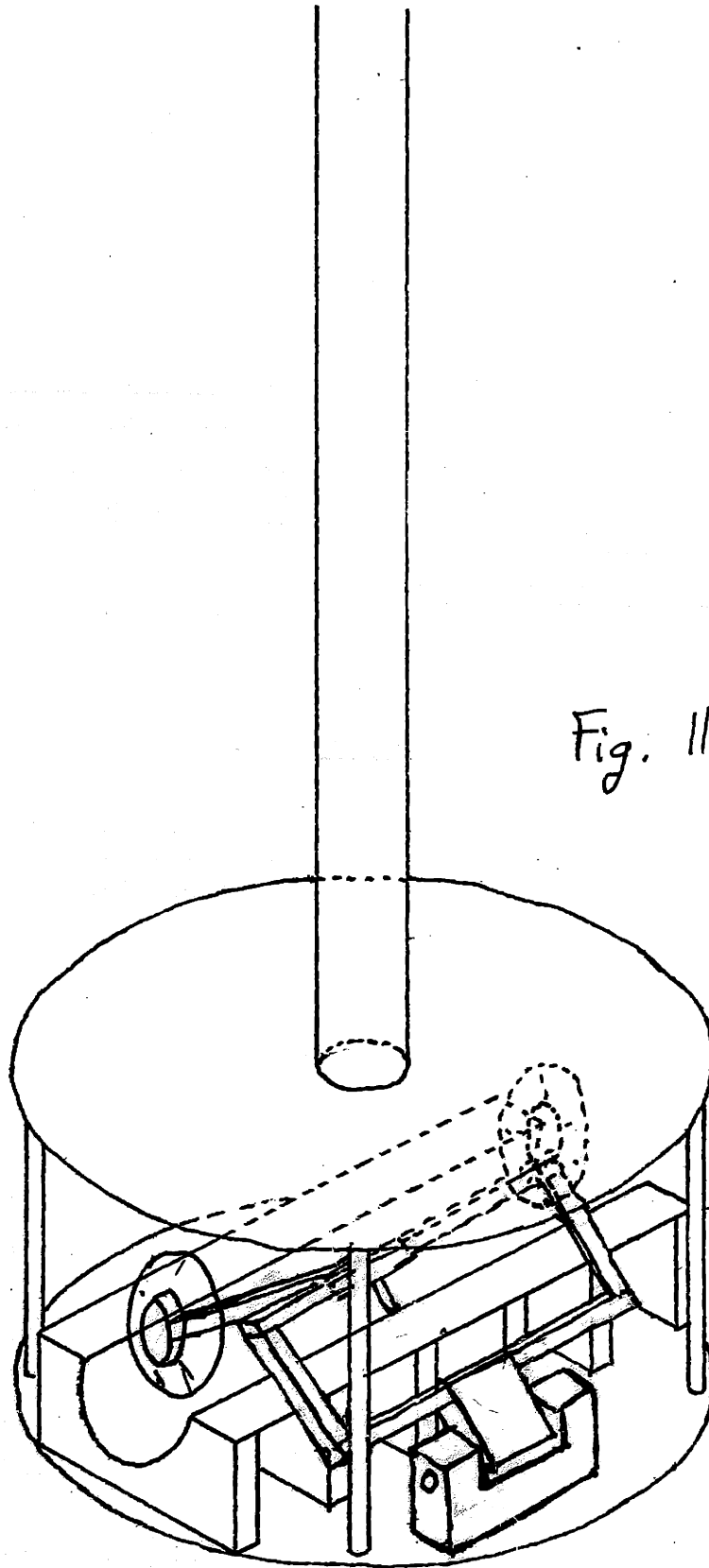


Fig. 11

than about 10 A. At this point, experimentation turned to contacts which were fastened to the coil, but could be pulled off. Indium proved to be the only solder soft enough at LHe temperatures. The contacts were constructed by welding a piece of Nb-Ti wire with part of its copper cladding etched off to each end of the coil. The external current leads were soldered to the remaining copper cladding. This arrangement was able to carry the requisite 25 A of current, but the method proved too cumbersome and never succeeded in floating the coil.

Force vs. Height and Current Experiment

Since the coil never floated in the previous trials, the possibility existed that a solenoid current of 25 A was insufficient to float the coil. Measurement of the force required an experimental set-up with the solenoid fixed to the base, and a trough suspended on a long wire above it (see fig.12). The long wire was hung from a spring scale mounted on a microscope stage on the top of the apparatus. The distance from the stationary solenoid to the hanging trough could be determined by combining the height reading from the microscope stage with the spring scale deflection:

$$d = M - H - 2.18 \text{ cm (offset)}$$

where  $d$  is the distance from solenoid to trough,  $M$  is the spring scale deflection in cm, and  $H$  is the microscope stage height in cm. Varying the height  $H$  and the persistent current  $I$  gave a measurement of the dependence of the Maxwell force on distance and current. The results of these measurements are graphed in figs. 13, 14, and 15.

As is apparent from fig. 15, the force scales very neatly with the square of the solenoid current up to about 20 A. At this point, the measured force falls significantly short of its projected value. This is probably not the result of changes from measurement to measurement, since the 25 A curves were measured several times, interspersed with readings at different currents. In addition, the scatter in the data points is small in comparison with an error of the requisite magnitude. The most probable explanation is that a 25 A persistent current never actually flowed in the solenoid. This would be the case if some link of the coil, perhaps the welds or the heater, had a small resistance at 25 A, but went completely superconducting at a current near 22 A.

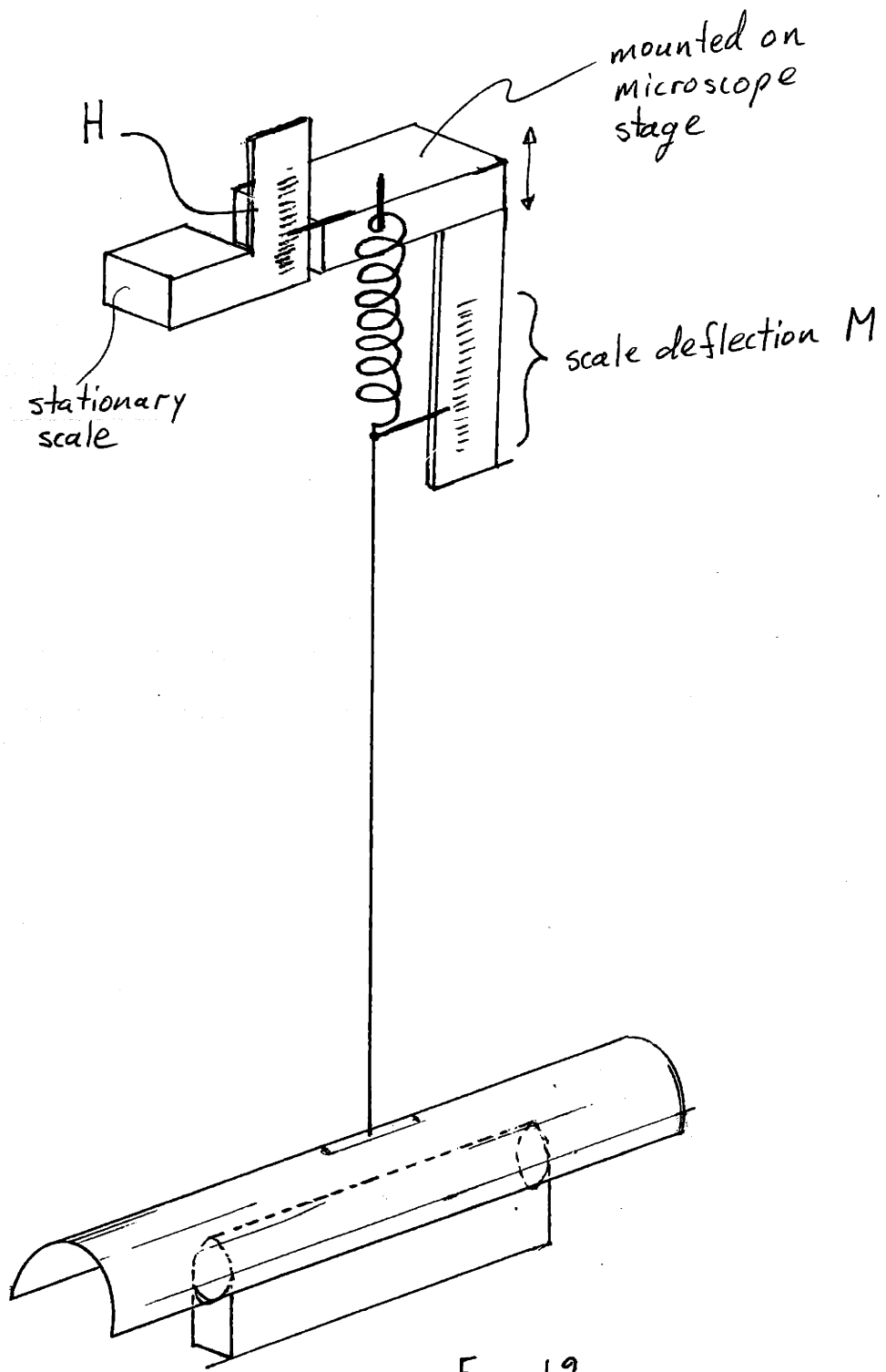


Fig. 12

• 1st run  
 ○ 2nd run  
 X 3rd run  
 ■ upper - line of dipoles reflected in plane  
 □ lower - line of dipoles " " V-shaped trough  
 ▲ upper } same as above, but with origin moved .8mm  
 ● lower } to the right.

Fig. 13

I = 25A

Force vs. distance from coil to trough

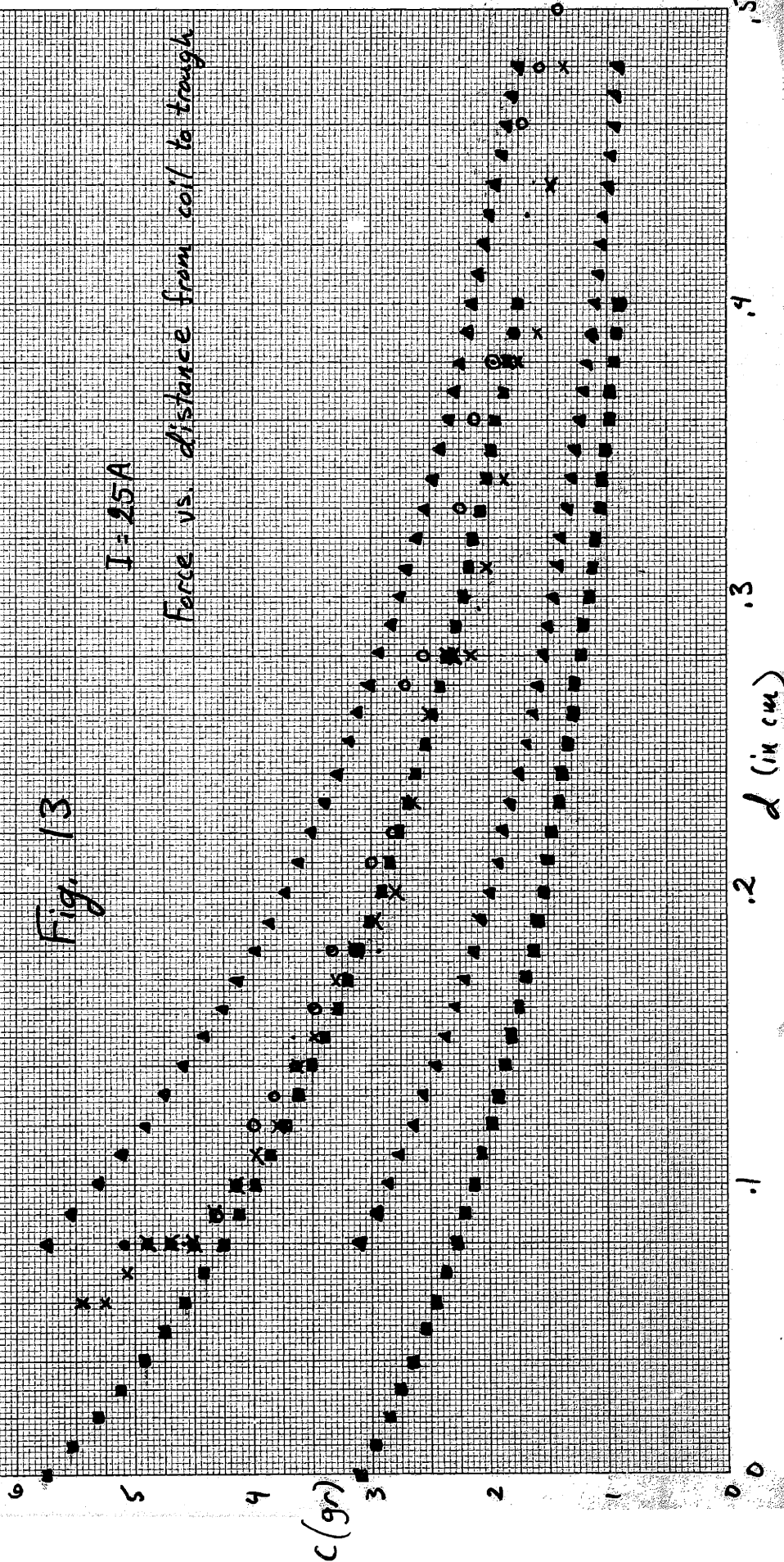


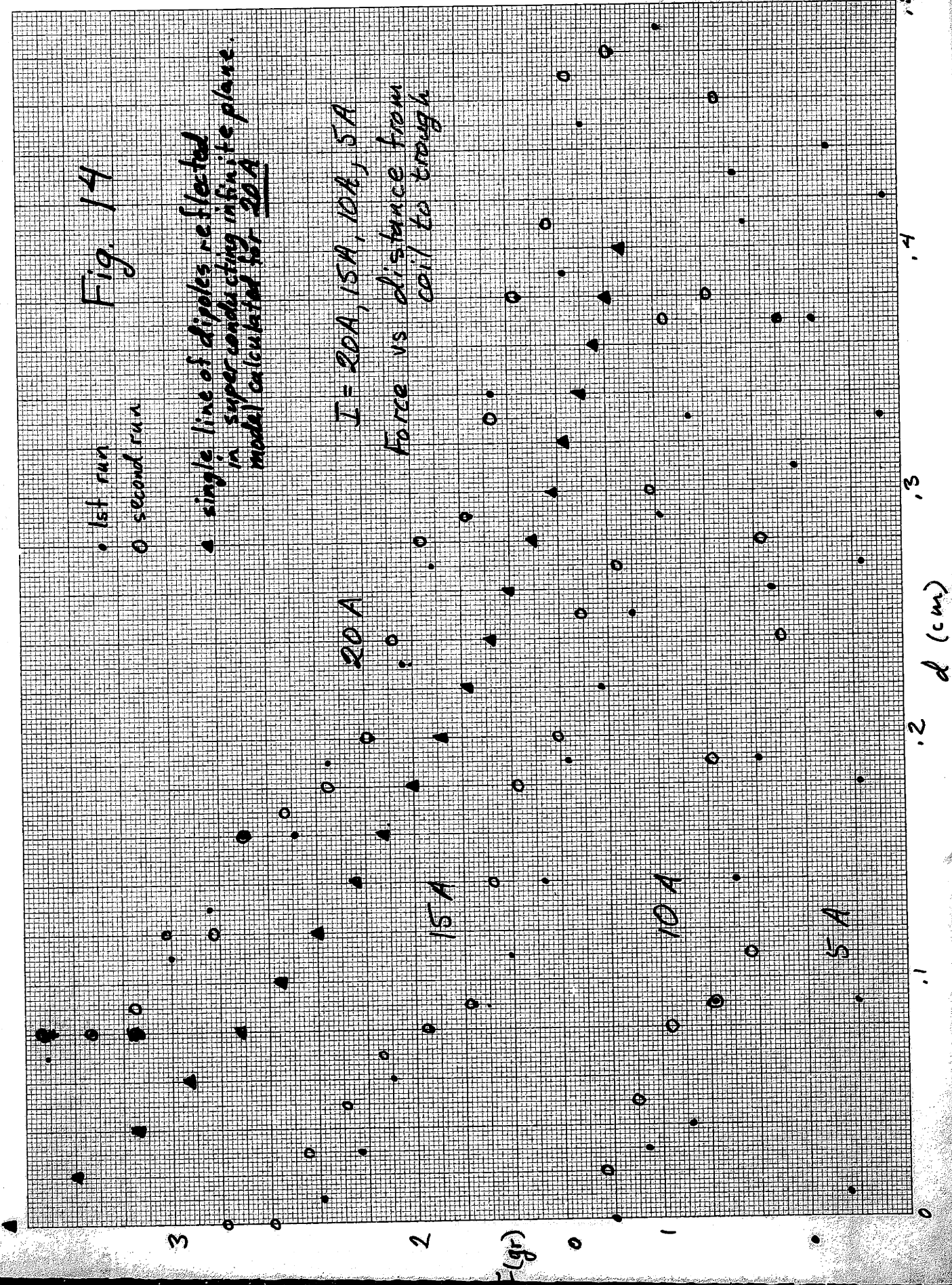
Fig. 14

• 1st run  
○ second run

a single line of dipoles reflected in superconducting infinite plane. model calculated for 20 A

I = 20 A, 15 A, 10 A, 5 A

Force vs distance from coil to trough

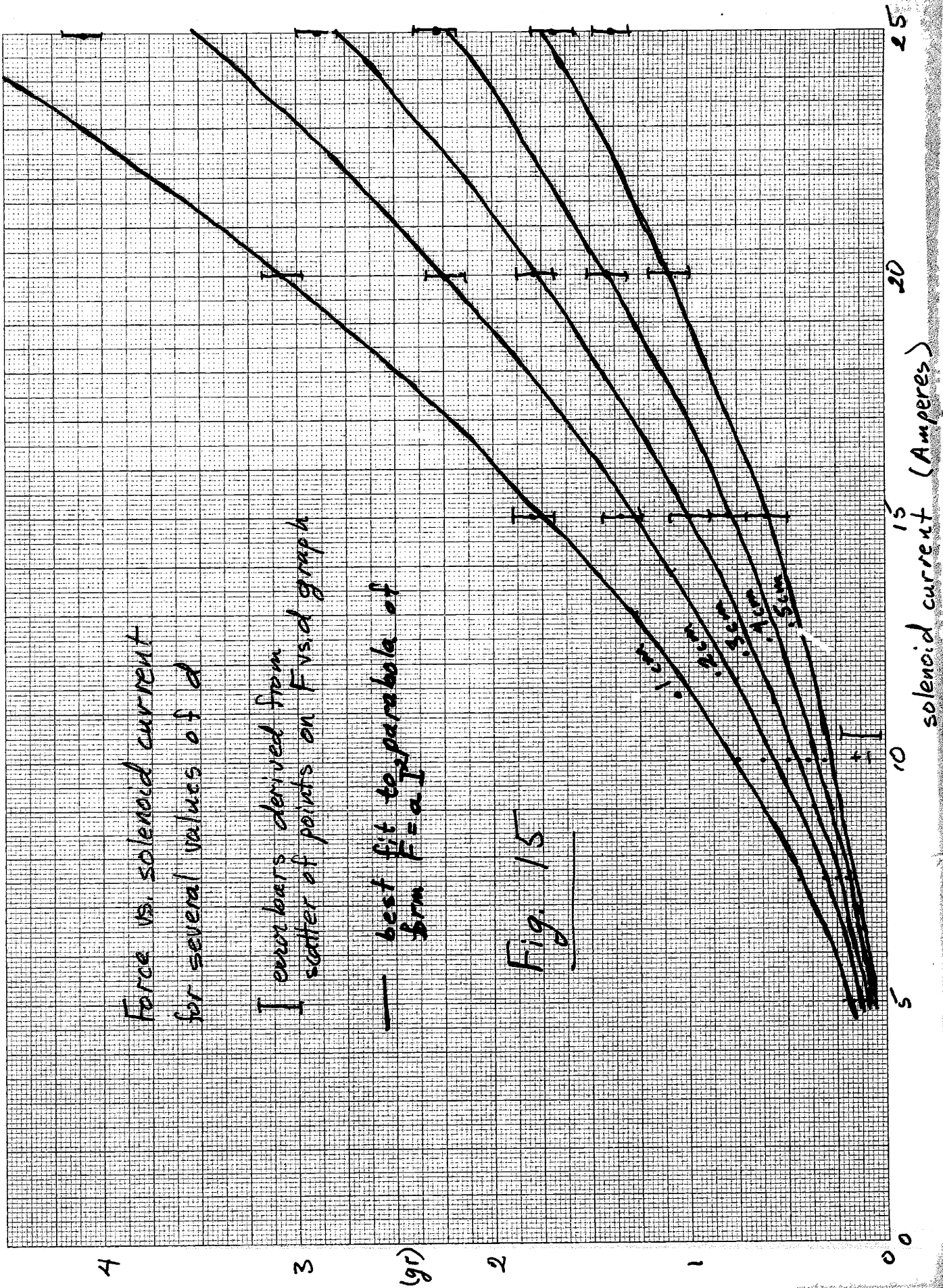


Force vs. solenoid current  
for several values of  $d$

I error bars derived from  
scatter of points on F vs  $d$  graph

— best fit to parabola of  
form  $F = aI^2$

Fig. 15



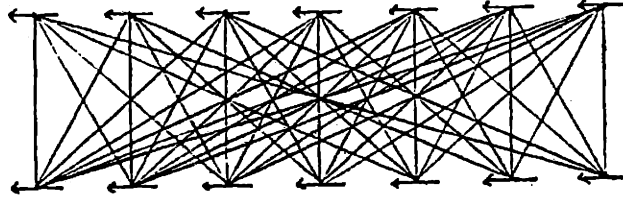


Fig. 16

RTII-V3 BASIC

```

5 PRINT 'INPUT S,K,N'
10 INPUT S,K,N
20 X1=4/N
30 FOR J=0 TO K
40 Z=1+2*J*S
45 F=0
50 FOR L=1 TO N
60 X=(L-1)*X1
70 A=(3*X^3-12*X*Z^2)/((X^2+Z^2)^(7/2))
80 IF L=1 THEN B=N
90 IF L>1 THEN B=2*(N+1-L)
100 F=F+A*B
110 NEXT L
120 M=156.99
130 F=(M/N)^2*F
140 PRINT Z,F
150 NEXT J
160 END

```

RTII-V3 BASIC

```

5 PRINT 'INPUT S,K,N'
10 INPUT S,K,N
20 X1=4/N
30 FOR J=0 TO K
40 Z=1+2*J*S
41 Z1=Z/SQR(2)
45 F=0
50 FOR L=1 TO N
60 X=(L-1)*X1
70 A=(3*X^3-12*X*Z^2)/((X^2+Z^2)^(7/2))
75 A1=(3*Z1^3-12*Z1*X^2)/((X^2+Z1^2)^(7/2))
80 IF L=1 THEN B=N
90 IF L>1 THEN B=2*(N+1-L)
100 F=F+A1*B*SQR(2)-A*B
110 NEXT L
120 M=156.99
130 F=(M/N)^2*F
131 H=(Z-1)/2
132 F1=F/990
140 PRINT H,F1
150 NEXT J
160 END

```

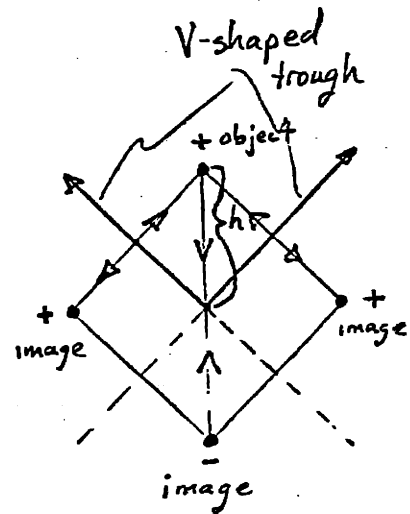


Fig. 18



Above 22 A, the power supply current would divide itself between the outer windings and the center link. The flux trapped in the coil would then tend to level off, and the force would no longer scale with the increasing supply current.

Since neither the single dipole model nor the spherical harmonic expansion provide an adequate description of the measured forces, some other model is necessary. The physical similarity between the long solenoid and a line of point dipoles suggests that the most fruitful approach involves approximating the coil-trough interaction as the force between two lines of dipoles. The total interaction may be calculated as the sum of the individual interactions between point dipoles. This process is shown schematically in fig. 16. From earlier calculations of dipole-dipole interactions:

$$\vec{B} = m_z \frac{3\cos^2\theta - 1}{r^3} \hat{z} + m_z \frac{3\cos\theta\sin\theta}{r^3} \hat{x}$$

Since, by symmetry, the transverse forces will cancel, it is only necessary to consider the vertical (x) forces. The x force is:

$$F_x = m_z \frac{\partial B_z}{\partial x} = m_z^2 \frac{\partial}{\partial x} \left( \frac{3\cos^2\theta - 1}{r^3} \right) = m_z^2 \frac{\partial}{\partial x} \left( \frac{2z^2 - x^2}{(x^2 + z^2)^{5/2}} \right)$$

where:

$$r = \sqrt{x^2 + z^2}, \quad \sin\theta = \frac{x}{\sqrt{x^2 + z^2}}, \quad \cos\theta = \frac{z}{\sqrt{x^2 + z^2}}$$

Carrying out the differentiation:

$$F_x = m_z^2 \frac{3x^3 - 12xz^2}{(x^2 + z^2)^{7/2}}$$

It is a relatively simple matter to write a computer program which sums these interactions after the fashion of fig. 16. A printout of

this program is in fig. 17. The curve resulting from this calculation converges rapidly as the number of dipoles in the line increases. The curves graphed with the data in figs. 13 and 14 are the results of calculations using lines of 80 dipoles (the number of turns in the solenoid).

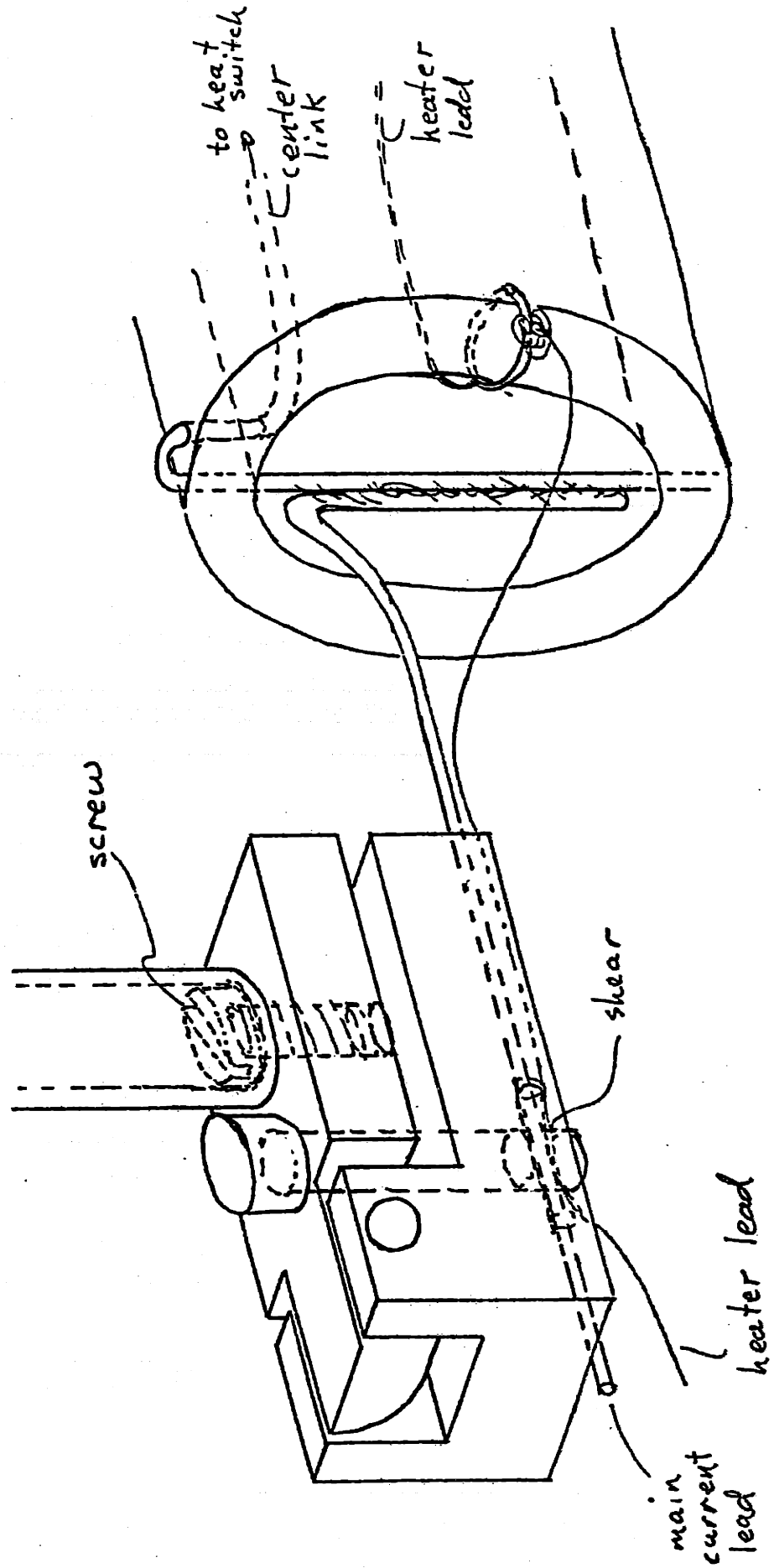
This curve is in excellent qualitative agreement with the data. By fudging the model in various ways (multiplying by a constant or shifting the origin), the model could be forced into numerical agreement with the data. The close agreement between the model calculations and the 25 A data is probably fortuitous, and it seems reasonable, in view of the glitch in the data at .8mm, to slide the origin of the calculation to the right. The lower curve is calculated by assuming the trough is equivalent to a  $90^\circ$  V-shaped groove. The interactions are again summed by computer in the manner shown schematically in fig. 18. This model gives forces which are much too small, but which remain in close qualitative agreement with the data. A numerically accurate model could probably be derived from general image considerations.

### Final Apparatus Design

The preceding experiment shows that the old coil is too heavy to be levitated by available currents. To lighten the new design, the center hole of the new form is larger, and is not filled with epoxy. This reduces the mass of the coil from about 5 gr to 2.682 gr. According to the previous measurements, 25 A should be ample to levitate the new coil. In addition, the new coil has 6 extra turns of Nb-Ti wire. This should increase the force by a factor of 1.15.

The second major change in the new set-up is the method of starting the persistent current. The new system incorporates wires which are soldered to terminals on the coil, and which are sheared off after the persistent current is established. The shears are operated from above with a long screwdriver. Fig. 19 is a detailed drawing of the coil and shears. These shears, though effective, are cumbersome to use. In preparation for each experiment, the clipped ends of the current wires from the previous experiment must be removed, and new leads soldered in their place. In addition, the current wires must be insulated from the shears. This is done by rolling 1/10 mil mylar around the around the current and heater wires. Two 5 cm lengths of clad Nb-Ti wire and 38 gauge magnet wire are first cut. Pre-curved mylar is then wound around parallel lengths of the two kinds of wire. The mylar is then rolled tightly by rolling between the fingers and poked through the wire hole in the shears. Finally, the current and heater leads are soldered to their respective connections on the ends of the coil and the leads from room temperature are soldered on the other end. The leads are then tested with an ohmmeter for shorts to the base and other leads.

Fig. 19



Under the assumption that the weld in the solenoid loop limits the the maximum current, the new welds have extra overlapping lengths of wire which provide a greater cross sectional area. The new current connections and the new welds carry more than 40 A when immersed in LHe. At this point, immersion tests confirmed that the coil would levitate.

Though the new coil levitated, it tended to squirt out the ends of the trough. To counteract this tendency, it was necessary to add disks of Niobium at the ends of the trough to repel the coil. Though this arrangement prevented the coil from squirting out the ends of the trough, it did not result in a single stable position for the coil. Instead, the coil could rest at either end of the trough, floating just clear of the end disks. Forcing a single stable position required the addition of a set of superconducting coils adjacent to the Niobium disks. These coils were connected in a closed loop containing a heat switch and enclosing a primary coil consisting of 50 turns of copper magnet wire. This arrangement allowed a persistent current to be established in the end coils which proved sufficient to force the coil to a single stable position in the middle of its travel. In addition, fluctuations in this persistent current caused by motions of the coil induced currents in the primary coil which could be used to deduce the velocity of the coil.

A long wire running longitudinally down the trough, close to the trough wall allowed the transverse modes of the system to be excited. This wire was hooked to leads from room temperature. The full arrangement is shown in fig. 20.

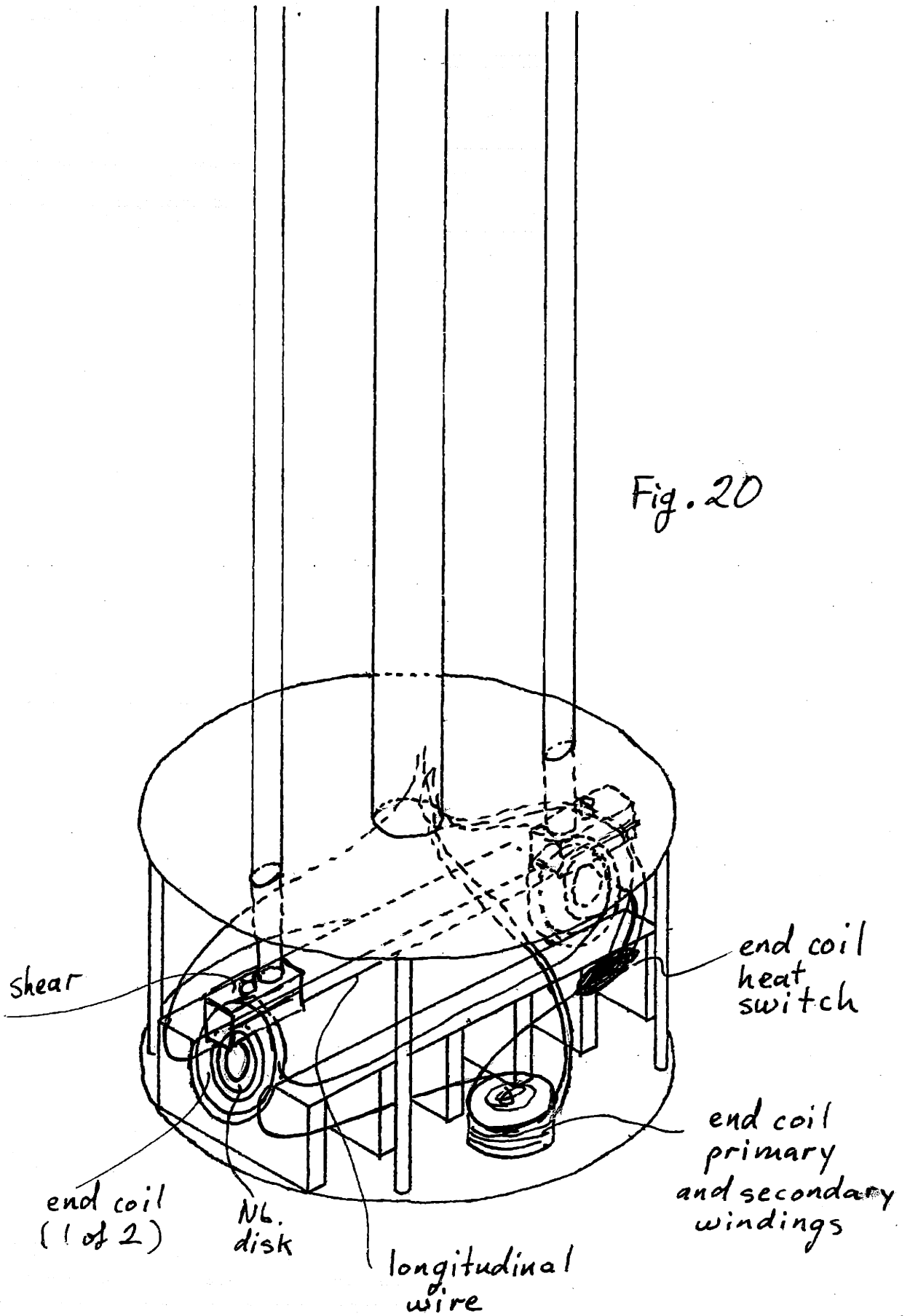


Fig. 20

### Resonance and Q Experiments

The following set of four experiments were intended to establish the Q and resonance frequencies of the suspended coil in the trough potential well. In the first, and least fruitful experiment, **neither** the end disks nor the end coils were in place. The coil floated, but hung itself up on the nylon thread used to keep it inside the trough. With a persistent current of 25 A (initial meter reading) the coil floated at a height of approximately 1.3mm. By shaking the LHe dewar, the up-down resonance could be excited. By using a stop-watch, and counting oscillations, the resonant frequency was measured as 5.5 Hz.

In the second experiment, **the** Niobium disks were added at the ends of the trough. These disks prevented the coil's escape, but did not force a single, stable coil position. The major results of this experiment were the transverse and rotational resonant frequencies of the system. The coil could be forced from one stable longitudinal position to another by bringing a bar magnet near the outer wall of the dewar. This magnet could also be used to excite longitudinal oscillations. The transverse resonances of the suspension were excited using the long wire running parallel to the wall of the trough. The current in this wire was controlled by a Wavetek signal generator. By adjusting the frequency of the signal generator and watching the coil response through the glass wall of the dewar, both the mode and resonance frequency could be determined. The modes and resonant frequencies are noted in table 4. A visual estimation of the system Q is about 20 to 30 in LHe. The LHe level decreased steadily throughout the experiment and eventually reached the level of the coil. The coil and trough remained superconducting even after the coil was completely

Table 4

mode	frequency	LHe or He gas	Q e= estimated	comments
↕	5.48 Hz.	LHe	20-30 e	
↓ □ ↑	8.62	LHe	"	
↻	.83	"	"	
⊙	5.40	"	"	appears to be combination of ↕ and ↔ modes.
□ ↔	2.70	LHe, He gas	20-30, 40-50 e	not single potential well
□ ↔	1.62	LHe	20-30 e	10 A
"	.67	"	"	12 A
"	.54	He gas	40-50 e	10.5 A
"	1.12	LHe	10-30	inertial damping
"		He gas	~65	viscous damping



exposed. It remained floating until the LHe level dropped below the bottom of the base plate. At this point, the trough itself probably went normal, since it is connected to room temperature by copper wires. A further line of investigation may be determination of the minimum He vapor pressure required to keep the coil superconducting. It is entirely possible that radiation cooling would prove sufficient if the coil were isolated from outside radiation.

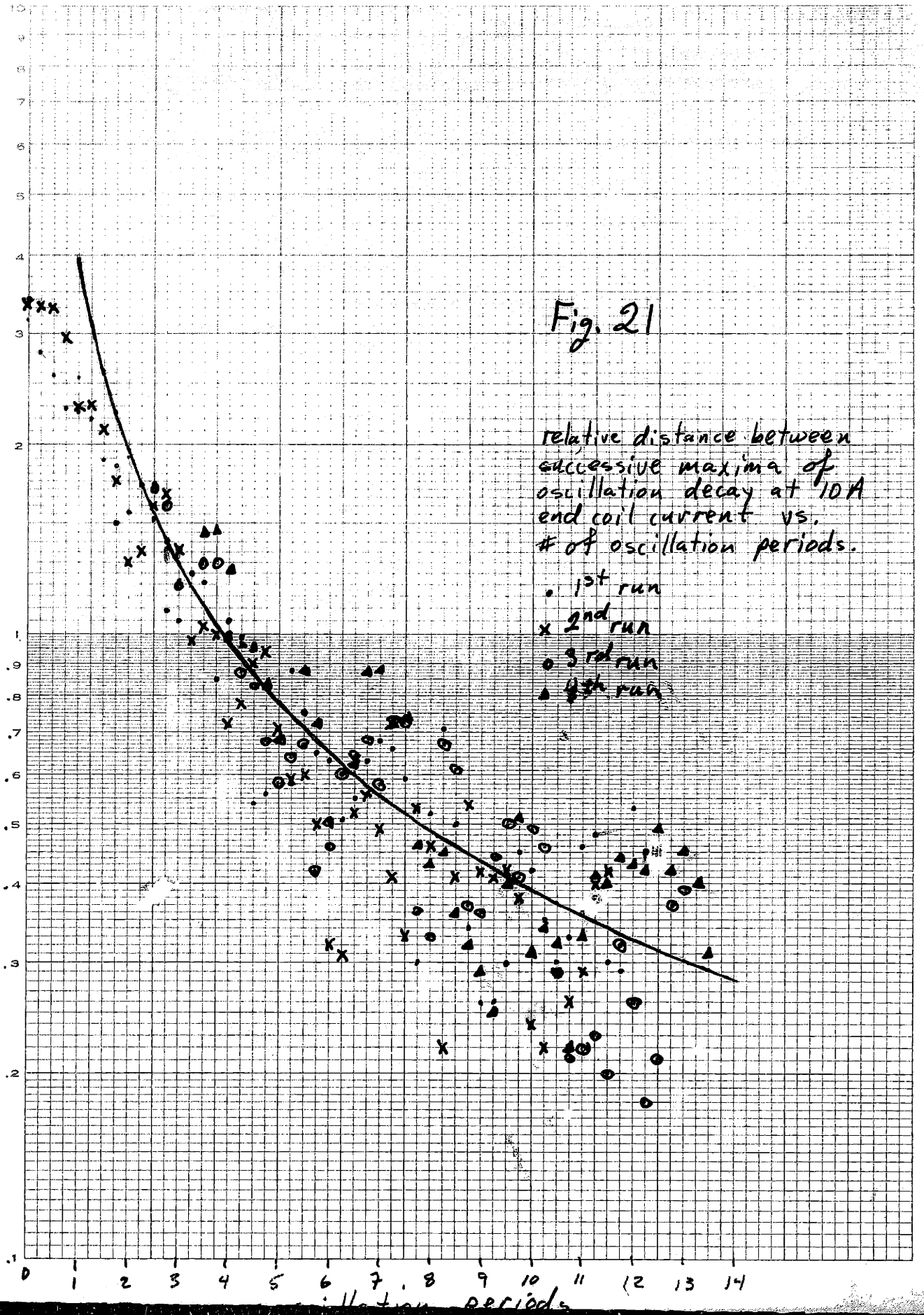
In the third experiment, the new end coils forced the solenoid to a stable, centered position. By adjusting the end coil current and the tilt of the trough, very low longitudinal oscillation frequencies could be obtained. These frequencies were again measured by clocking the oscillations with a stopwatch. The resonance frequencies from this experiment are tabulated in table 4. Visually estimated Q's are again about 20 or 30 in LHe, and 40 to 50 in He gas.

The fourth and final experiment was an attempt to measure the Q of the longitudinal mode. In this experiment, an end coil current of 10 or 12 A confines the solenoid to its stable position, and fluctuations in this current due to motion of the solenoid induce a sense voltage dependent on its velocity and position. This voltage, after amplification and filtering, produces a trace on a strip-chart recorder. Since the sense voltage depends on both the velocity and position of the solenoid, a single cycle of oscillation produces two cycles in the sense voltage, corresponding to an increase and decrease of the field seen by the two end coils. The data from this measurement is analyzed in terms of successive peak-to-peak measurements of the sense voltage amplitude. This produces four data points for each oscillation of the solenoid. The oscillations are initiated by jogging the coil with an external

magnet. The data shown in figs. 21, 22, and 23 are the combinations of 4 decay curves at 10 and 12 A end coil current and 2 decays at 12 A with the coil moving in gaseous He. Unfortunately, the noise in the amplifiers makes any detail of the decay, but the semi-log plots still give a rough idea of the respective Q's.

DIETZGEN CORPORATION  
MADE IN U.S.A.

NO. 340-L210 DIETZGEN GRAPH PAPER  
SEMI-LOGARITHMIC  
2 CYCLES X 10 DIVISIONS PER INCH



DIETZGEN CORPORATION  
MADE IN U.S.A.

NO. 340-L210 DIETZGEN GRAPH PAPER  
SEMI-LOGARITHMIC  
2 CYCLES X 10 DIVISIONS PER INCH

relative  
amplitude

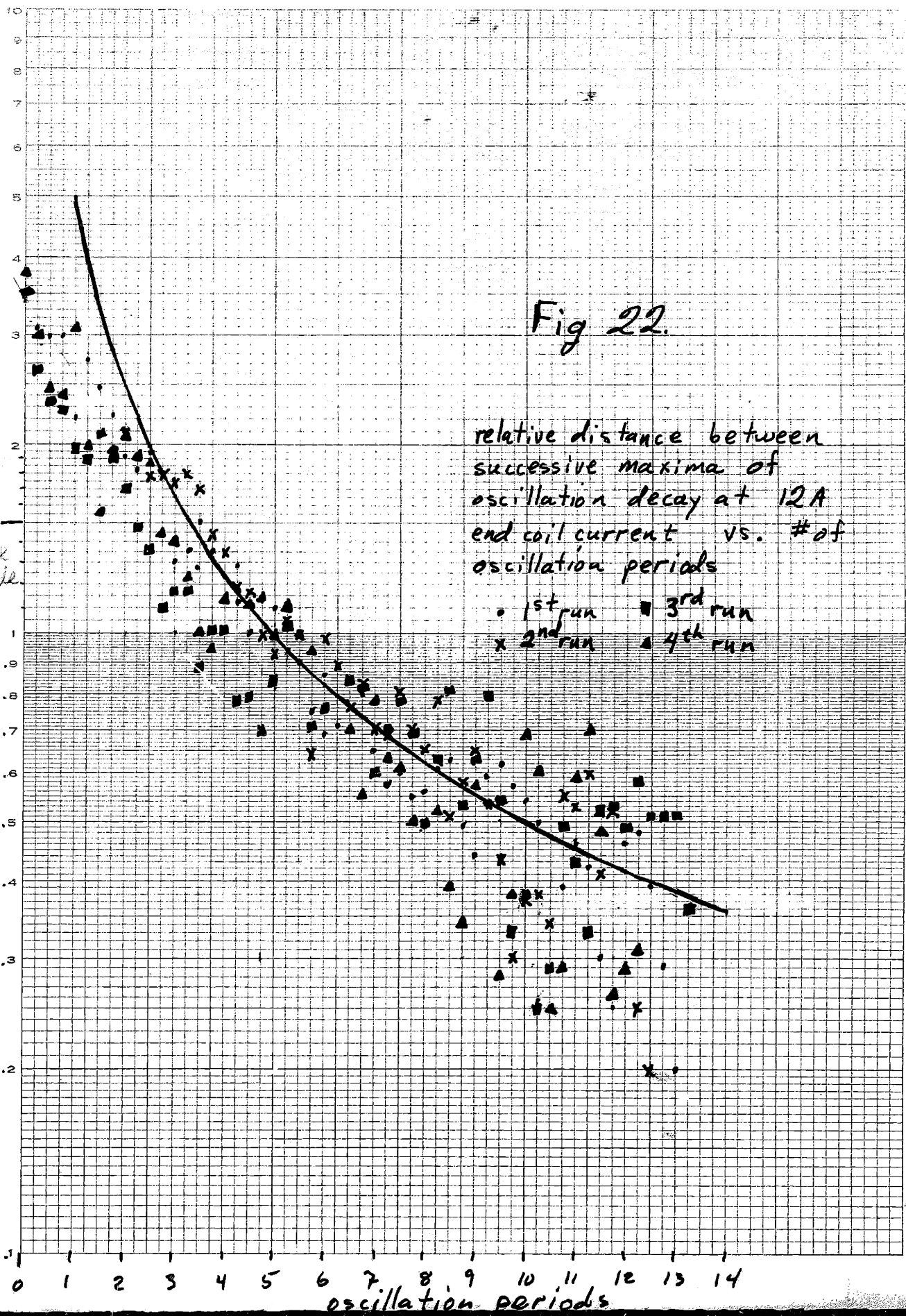


Fig 22.

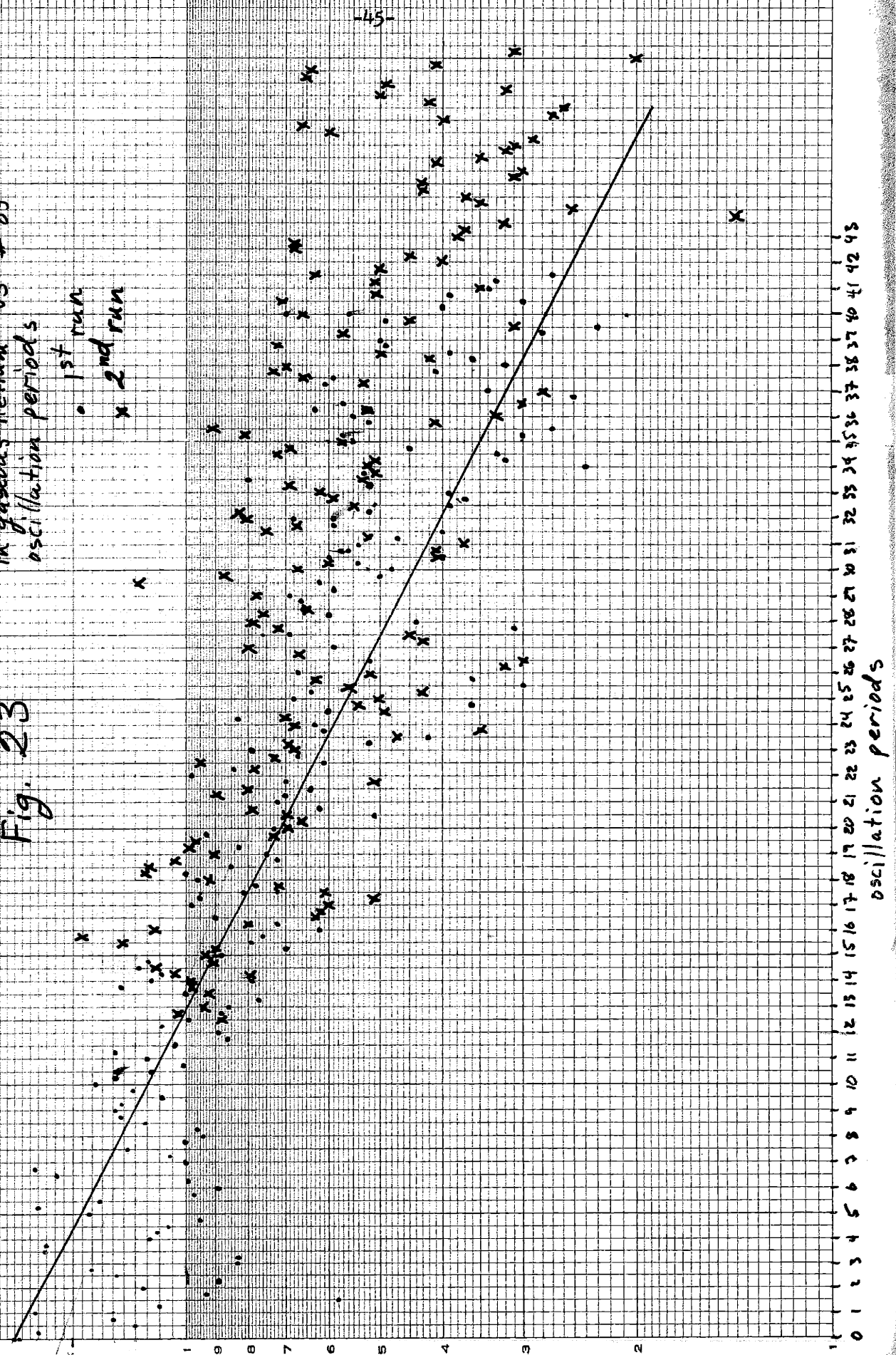
201

relative distance between successive maxima of oscillation decay at 12A end coil current in gaseous Helium vs # of oscillation periods

• 1st run  
x 2nd run

$\nu_0 \approx 1.03 \text{ Hz}$

Fig. 23



Q and Resonance Data Analysis

The resonant frequencies of the suspension give the force constants appropriate to their respective modes of oscillation via the expression:

$$\omega = \sqrt{\frac{k}{m}}, \quad k = m\omega^2 = 4\pi^2\nu^2 m$$

For all except the vertical mode, the resonant frequencies are the only measure of the confining forces. The vertical confining force has, however, been measured separately, and the corresponding resonance frequency should match the measured value. From the 25 A force vs. distance graph, the slope at a coil distance of .4 cm (taking the origin to be .08 cm) is:

$$\frac{dF}{dz} \approx 1.8 \text{ gr/cm} \longrightarrow k = 1764 \text{ dyne/cm}$$

Scaling the force up to 2.682 gm x 980 dyne/gm gives k=3218 dyne/cm.

This gives:

$$\nu = \frac{1}{2\pi} \sqrt{\frac{k}{m}} = 5.5 \text{ Hz}, \quad m = 2.682 \text{ gr},$$

which is very close to the measured value of 5.48 Hz. This indicates that the experiment is at least internally consistent.

The liquid or gaseous He surrounding the solenoid damps oscillations via some velocity dependent force. The velocity dependence of this force should be roughly predictable from the characteristics of the helium fluid. The inertial damping force results from the rate of momentum transfer from the solenoid to the fluid it displaces.

The momentum transfer per unit volume is:

$$\frac{\Delta p}{\text{vol.}} = \rho u$$

The volume affected per unit time is:

$$\frac{\Delta v}{\Delta t} = 2Au$$

where A is the effective cross-sectional area of the solenoid. The inertial damping force is therefore:

$$F_{\text{inertial}} = 2\rho Au^2 \propto u^2$$

The viscous damping force is given by<sup>4</sup>:

$$F_{\text{viscous}} = \eta \frac{du}{dz} A$$

where  $\eta$  is the viscosity, and  $z$  is a direction perpendicular to the line of motion. The velocity gradient is approximately:

$$\frac{du}{dz} \approx \frac{u}{r}$$

where  $r$  is the effective radius of the solenoid. The viscous force is therefore:

$$F_{\text{visc.}} \approx \eta \frac{u}{r} A$$

The Reynolds number of the flow is the ratio of the inertial to the viscous force. A Reynolds number greater than 500-1000 implies the damping is mostly inertial, while a lesser value implies mostly viscous damping. The Reynolds number is:

$$R \approx \frac{2\rho Au^2}{\eta u/r A} = \frac{2\rho r u}{\eta}$$

Plugging in values for LHe gives:

$$R = \frac{2 \cdot .149 \text{ gm/cc} \cdot .15 \text{ cm} \cdot \omega x}{3.6 \times 10^{-5} \rho} \approx 1.2 \times 10^3 \omega x$$

The measured frequency is approximately 1 Hz., and the approximate initial amplitude is  $\sim 1.5$  cm. This gives  $\omega x \approx 9.4$  cm/sec. This gives:

$$R \approx 1.1 \times 10^4$$

which implies the damping force is virtually all inertial. On the other hand, in gaseous He:

$$R \approx \frac{2 \cdot .012 \text{ gm/cc} \cdot .15 \text{ cm} \cdot \omega x}{10^{-5} \rho} = 360 \omega x \approx 2.4 \times 10^3$$

which is marginal, so the damping could be a combination of both inertial and viscous damping.

The actual measurement of the amplitude decay rate is complicated by the amplitude dependence of the sense coil voltage. Since the sense coil is less sensitive to the solenoid velocity at smaller oscillation

amplitudes, the oscillations will seem to damp more quickly, and the slope of the semi-log plots (figs. 21, 22, and 23) will underestimate the system Q. The following analysis assumes that this effect is small due to the channeling effect of the Niobium trough.

The full analytic behavior of oscillations subject to a quadratic velocity damping force follows the differential equation:

$$\frac{dx^2}{dt^2} + \frac{\alpha}{m} \left( \frac{dx}{dt} \right)^2 + \omega_0^2 x = 0$$

Since the data is so noisy, solution of this equation would be a waste of time. Instead, the energy loss per cycle is calculated using sinusoidal oscillations. The energy loss per cycle is:

$$\Delta E = 4\alpha \int_0^{T/4} A^3 \omega^3 (\cos^2 \omega t) \cos \omega t dt = \frac{4\alpha A^3 \omega^3 T}{3\pi}$$

The average rate of energy loss is therefore:

$$\frac{dE}{dt} \approx - \frac{4\alpha A^3 \omega^3}{3\pi}$$

The energy stored is:

$$E = \frac{1}{2} m \dot{x}^2 = \frac{1}{2} m A^2 \omega^2$$

The rate of change of the amplitude is:

$$\frac{dA}{dt} = \frac{dA}{dE} \frac{dE}{dt} = - \frac{4\alpha A^2 \omega^3}{3\pi m A \omega^2} = - \frac{4\alpha A \omega}{3\pi m}$$

Integrating gives:

$$\int \frac{dA}{A^2} = - \int \frac{4\alpha \omega}{3\pi m} dt = - \frac{1}{A} = - \frac{4\alpha \omega}{3\pi m} t$$

Therefore:

$$A = \frac{3\pi m}{4\alpha \omega t} = \frac{3m}{8\alpha} \left( \frac{T}{t} \right)$$

Since this approximation assumes a constant amplitude over a cycle, it



should break down at high amplitudes where losses are high. The black line drawn on figs. 21 and 22 is a qualitative (eyeball) fit to a  $1/t$  curve. Assuming that the position dependence of the velocity sensor is small, this fit tends to verify the inertial character of the damping. The damping curve in fig. 23, however, has no evidence of a  $1/t$  dependence, and fits (roughly) to a straight line. The slope of the line is  $-4.756 \times 10^{-2} \times 1/T$ , which gives a Q of:

$$Q = \frac{\omega}{\delta} = \frac{2\pi/T}{\frac{2.4756 \times 10^{-2}}{T}} = 66$$

Since the motion in gaseous He appears viscously damped, it is possible to set a lower limit on the maximum viscously damped amplitude in LHe. By forcing the Reynolds numbers for the two cases to match, the maximum A in LHe is  $\sim 2$ cm.

### Conclusions

It is possible to levitate a small superconducting solenoid on its own magnetic field with conveniently producible persistent currents. The mechanism described in this paper for establishing that current is, however, cumbersome and inconvenient. The apparatus must be withdrawn from the LHe, dismantled, reassembled, and re-cooled before a new persistent current can be established. It also lacks reliability in that about half the attempts to start a persistent current fail. Some sort of pressure contact is clearly desirable.

The magnetic interaction between the coil and the trough can be modeled as the repulsive force between two long lines of point dipoles. This model describes the data up to a multiplicative factor.

Once floating, the solenoid can be confined in the Nb trough so that its longitudinal resonance frequency is in the neighborhood of 1 Hz. This value can probably be reduced by a more elaborate confinement system. This resonance has a Q of about 10 for 3 cm peak-to-peak motion in LHe, increasing to about 40 at amplitudes less than .3 cm. In gaseous He, the Q is about 65.

The damping force in LHe is inertial, while the damping in gaseous He is viscous. With peak-to-peak amplitudes less than about .2 cm, the damping force in LHe should also be viscous (for 1 Hz. frequency).

Since the solenoid remains superconducting in He gas, it may be possible to evacuate the apparatus and cool the solenoid radiatively (after the persistent current is established). This should **increase the Q** drastically.

Blair<sup>5</sup> has described a superconducting accelerometer which consists of a thin Nb tube supported by a current carrying wire through its center.

This geometry has the advantage that the test mass is entirely passive.

Acknowledgements

I wish to give my sincere thanks to Prof. Rainer Weiss for his continual support and quick insight, to Dick Benford for his technical advice, and to P. Kramer, P. Downey, M. Halpern, D. Shoemaker, and A. Jeffries for their helpful comments and criticisms. Also, I thank the Magnetic Corporation of America for the donation of the superconducting wire, and G. Leach for the use of his facilities.

References

1. Ezekiel, S., Masters Thesis, Electrical Engineering, M.I.T., 1967
2. Newhouse, Vernon, L., Applied Superconductivity, John Wiley Sons, N.Y., 1964.
3. Magnetic Corporation of America, private communication.
4. Newman, F.H. and Searle V. H., The General Properties of Matter, Edward Arnold (Publisher), London, 1957.
5. Blair, David G., Superconducting Accelerometer Using Niobium on Sapphire Resonator, Review of Scientific Instruments, 50(3), Mar. 1979.
6. Jackson, John D., Classical Electrodynamics, John Wiley & Sons, N.Y., 1962.